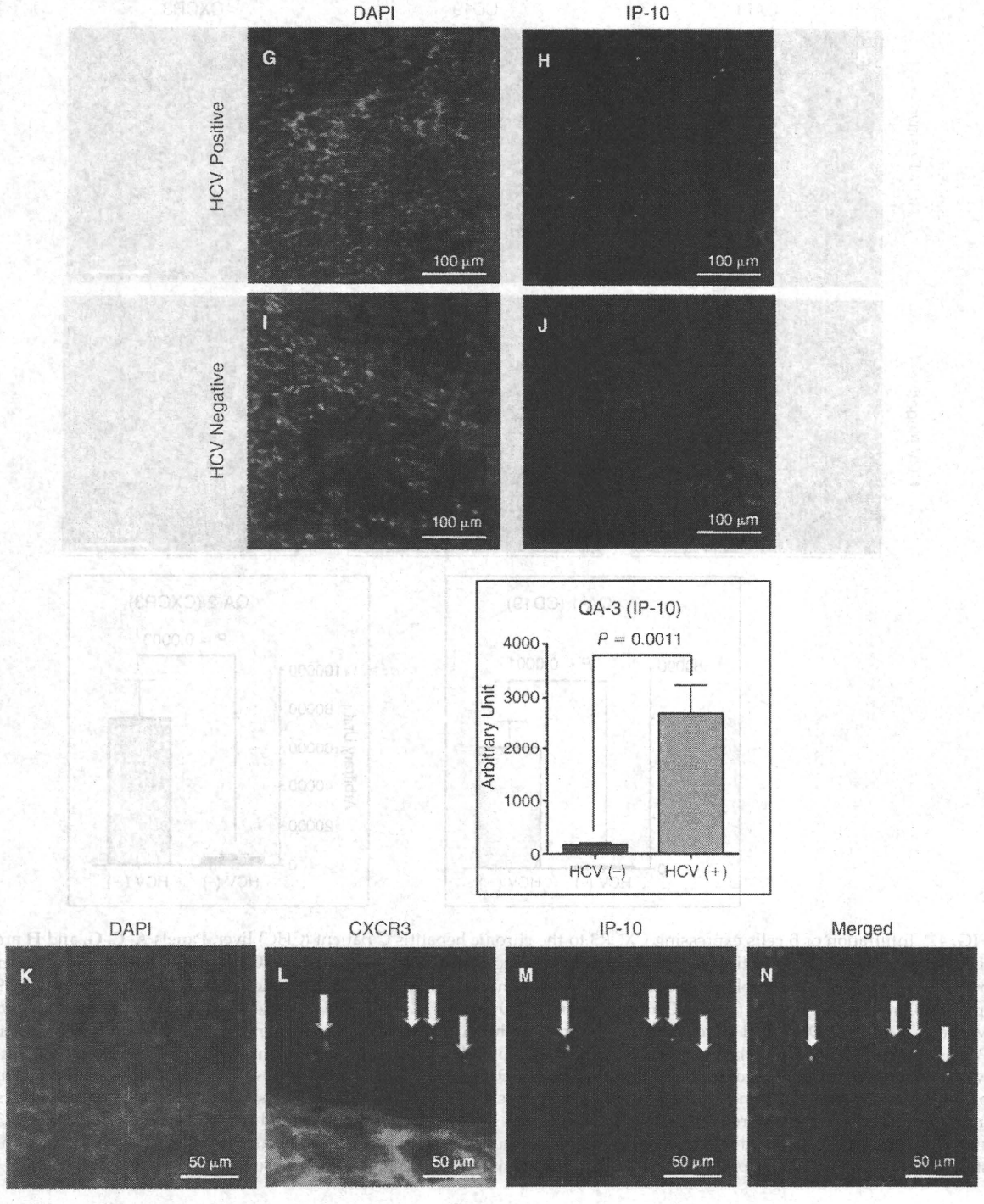

FIG. 4. *(Continued)*

Furthermore, in the inflamed tissue, inflammatory cytokines and autoantigens provide survival signals that promote plasma cell differentiation and survival, which may result in chronic inflammation and progressive tissue destruction. The present results are in line with this scenario when the HCV E2 protein is regarded as an autoantigen.

MC, a chronic autoimmune disorder, is usually associated with chronic liver inflammation by HCV infection (Dore and others 2007; Galossi and others 2007; Zignego and others 2007). Excessive production of antibodies known as RF is the main cause of MC. The fact that the majority of circulating B cells of patients with HCV-associated MC are

of the CD27+ phenotype (Carbonari and others 2005) further supports the contribution of memory B cells to extrahepatic autoimmune disorders.

Migration of B cells expressing CXCR3 into the CHC liver

In order to directly assess the migration of B cells expressing CXCR3 to the liver, immunohistochemical analyses were carried out by staining liver biopsy specimens. Unfortunately, as we could not obtain the biopsy specimens from the CHC analyzed in the above experiments, they were collected from other chronic hepatitis C patients. Liver biopsy specimens of alcohol-induced HCV-negative hepatitis patients instead of normal subjects were used as controls, since we could not obtain normal liver biopsy specimens.

As shown in Figure 4, the infiltration of CD19+ B cells were recognized in the liver of a HCV-positive hepatitis C patient, and the distribution of the CD19+ cells in the liver was almost identical to that of CXCR3+ cells (panels B vs. C). These CXCR3+ B-cell infiltrations were not observed in an HCV-negative alcohol-induced hepatitis patient specimen (panels E and F). Five HCV-positive and three HCV-negative independent liver biopsy specimens were analyzed, and similar staining profiles as shown in the figure were obtained. As expected, IP-10 was expressed in the liver of a CHC (panel H) but not in an HCV-negative specimen (panel J). Figure 4K–4N indicated that CXCR3+ cells are localized at the sites where IP-10 is expressed positive. Together, these results are concordant with our hypothesis that CD27+ B cells expressing CXCR3 migrate into the liver of PIP.

In this study, it was demonstrated that significant reductions in peripheral CD27+ B cells are seen in CHC, while plasma levels of IP-10, a CXCR3 ligand, are markedly increased in CHC. Furthermore, it was found that the CD27+ B cells highly express the CXCR3. In accordance with these phenomena, immunohistochemical analyses revealed that CXCR3+ B cells migrate in the liver of CHC where IP-10 is produced.

Finally, it is worth mentioning here that the recruitment of peripheral memory B cells into inflamed tissue may not be unique to CHC but rather is a general phenomenon. A recent report by Hansen et al. showed accumulation of memory B cells in the inflamed salivary glands of Sjoegren's syndrome patients (Hansen and others 2002), and Malbran et al. found that peripheral CD27+ memory B cells are reduced in patients with X-linked lymphoproliferative disease (Malbran and others 2004). Further investigation into the dynamics of memory B cells in chronically HCV-infected patients will be necessary, not only to better understand the HCV pathogenesis in particular, but also to gain insight into immunological disorders such as tolerance breakdown in general.

Acknowledgments

We are grateful to Dr. Masayuki Saijo for multiplex suspension bead array immunoassay and for operation of the Luminex analyzer. We would also like to thank Ms. Tomoko Nagai for immunohistochemical staining, and Dr. Yoshimasa Takahashi for valuable discussion and critical review of the manuscript. This study was supported by Grants-in-Aid from the Ministry of Health, Labor, and Welfare.

Author Disclosure Statement

The authors have no conflicting financial interests.

References

Agematsu K, Hokibara S, Nagumo H, Komiyama A. 2000. CD27: a memory B-cell marker. Immunol Today 21(5):204–206.

Carbonari M, Caprini E, Tedesco T, Mazzetta F, Tocco V, Casato M, Russo G, Fiorilli M. 2005. Hepatitis C virus drives the unconstrained monoclonal expansion of VH1-69-expressing memory B cells in type II cryoglobulinemia: a model of infection-driven lymphomagenesis. J Immunol 174(10):6532–6539.

Dammacco F, Sansonno D, Piccoli C, Racanelli V, D'Amore FP, Lauletta G. 2000. The lymphoid system in hepatitis C virus infection: autoimmunity, mixed cryoglobulinemia, and Overt B-cell malignancy. Semin Liver Dis 20(2):143–157.

Dore MP, Fattovich G, Sepulveda AR, Realdi G. 2007. Cryoglobulinemia related to hepatitis C virus infection. Dig Dis Sci 52(4):897–907.

Galossi A, Guarisco R, Bellis L, Puoti C. 2007. Extrahepatic manifestations of chronic HCV infection. J Gastrointestin Liver Dis 16(1):65–73.

Hansen A, Odendahl M, Reiter K, Jacobi AM, Feist E, Scholze J, Burmester GR, Lipsky PE, Dorner T. 2002. Diminished peripheral blood memory B cells and accumulation of memory B cells in the salivary glands of patients with Sjogren's syndrome. Arthritis Rheum 46(8):2160–2171.

Itoh Y, Morita A, Nishioji K, Narumi S, Toyama T, Daimon Y, Nakamura H, Kirishima T, Okanoue T. 2001. Clinical significance of elevated serum interferon- inducible protein-10 levels in hepatitis C virus carriers with persistently normal serum transaminase levels. J Viral Hepat 8(5):341–348.

Lauer GM, Walker BD. 2001. Hepatitis C virus infection. N Engl J Med 345(1):41–52.

Levy S, Todd SC, Maecker HT. 1998. CD81 (TAPA-1): a molecule involved in signal transduction and cell adhesion in the immune system. Annu Rev Immunol 16:89–109.

Machida K, Cheng KT, Lai CK, Jeng KS, Sung VM, Lai MM. 2006. Hepatitis C virus triggers mitochondrial permeability transition with production of reactive oxygen species, leading to DNA damage and STAT3 activation. J Virol 80(14):7199–7207.

Machida K, Cheng KT, Pavio N, Sung VM, Lai MM. 2005. Hepatitis C virus E2-CD81 interaction induces hypermutation of the immunoglobulin gene in B cells. J Virol 79(13):8079–8089.

Machida K, Cheng KT, Sung VM, Lee KJ, Levine AM, Lai MM. 2004. Hepatitis C virus infection activates the immunologic (type II) isoform of nitric oxide synthase and thereby enhances DNA damage and mutations of cellular genes. J Virol 78(16):8835–8843.

Malbran A, Belmonte L, Ruibal-Ares B, Bare P, Massud I, Parodi C, Felippo M, Hodinka R, Haines K, Nichols KE, de Bracco MM. 2004. Loss of circulating CD27+ memory B cells and CCR4+ T cells occurring in association with elevated EBV loads in XLP patients surviving primary EBV infection. Blood 103(5):1625–1631.

Manz RA, Moser K, Burmester GR, Radbruch A, Hiepe F. 2006. Immunological memory stabilizing autoreactivity. Curr Top Microbiol Immunol 305:241–257.

Muehlinghaus G, Cigliano L, Huehn S, Peddinghaus A, Leyendeckers H, Hauser AE, Hiepe F, Radbruch A, Arce S, Manz RA. 2005. Regulation of CXCR3 and CXCR4 expression during terminal differentiation of memory B cells into plasma cells. Blood 105(10):3965–3971.

Narumi S, Tominaga Y, Tamaru M, Shimai S, Okumura H, Nishioji K, Itoh Y, Okanoue T. 1997. Expression of IFN-inducible protein-10 in chronic hepatitis. J Immunol 158(11):5536–5544.

Ni J, Hembrador E, Di Bisceglie AM, Jacobson IM, Talal AH, Butera D, Rice CM, Chambers TJ, Dustin LB. 2003. Accumulation of B lymphocytes with a naive, resting phenotype in a subset of hepatitis C patients. J Immunol 170(6):3429–3439.

Ohno O, Mizokami M, Wu RR, Saleh MG, Ohba K, Orito E, Mukaide M, Williams R, Lau JY. 1997. New hepatitis C virus (HCV) genotyping system that allows for identification of HCV genotypes 1a, 1b, 2a, 2b, 3a, 3b, 4, 5a, and 6a. J Clin Microbiol 35(1):201–207.

Pal S, Sullivan DG, Kim S, Lai KK, Kae J, Cotler SJ, Carithers RL, Jr., Wood BL, Perkins JD, Gretch DR. 2006. Productive replication of hepatitis C virus in perihepatic lymph nodes *in vivo*: implications of HCV lymphotropism. Gastroenterology 130(4):1107–1116.

Patzwahl R, Meier V, Ramadori G, Mihm S. 2001. Enhanced expression of interferon-regulated genes in the liver of patients with chronic hepatitis C virus infection: detection by suppression-subtractive hybridization. J Virol 75(3):1332–1338.

Pileri P, Uematsu Y, Campagnoli S, Galli G, Falugi F, Petracca R, Weiner AJ, Houghton M, Rosa D, Grandi G, Abrignani S. 1998. Binding of hepatitis C virus to CD81. Science 282(5390):938–941.

Racanelli V, Frassanito MA, Leone P, Galiano M, De Re V, Silvestris F, Dammacco F. 2006. Antibody production and in vitro behavior of CD27-defined B-cell subsets: persistent hepatitis C virus infection changes the rules. J Virol 80(8):3923–3934.

Rosa D, Saletti G, De Gregorio E, Zorat F, Comar C, D'Oro U, Nuti S, Houghton M, Barnaba V, Pozzato G, Abrignani S. 2005. Activation of naive B lymphocytes via CD81, a pathogenetic mechanism for hepatitis C virus-associated B lymphocyte disorders. Proc Natl Acad Sci USA 102(51):18544–18549.

Vallat L, Benhamou Y, Gutierrez M, Ghillani P, Hercher C, Thibault V, Charlotte F, Piette JC, Poynard T, Merle-Beral H, Davi F, Cacoub P. 2004. Clonal B cell populations in the blood and liver of patients with chronic hepatitis C virus infection. Arthritis Rheum 50(11):3668–3678.

Zignego AL, Giannini C, Ferri C. 2007. Hepatitis C virus-related lymphoproliferative disorders: an overview. World J Gastroenterol 13(17):2467–2478.

Address correspondence to:
Dr. Toshiaki Mizuochi
Department of Research on Blood and Biological Products
National Institute of Infectious Diseases
4-7-1 Gakuen Musashimurayama
Tokyo 208-0011
Japan

E-mail: miz@nih.go.jp

Received 14 May 2009/Accepted 23 July 2009

Clinica Chimica Acta 411 (2010) 605–606

Contents lists available at ScienceDirect

Clinica Chimica Acta

journal homepage: www.elsevier.com/locate/clinchim

Letter to the Editor

Single amino acid substitution in the hepatitis B virus surface antigen (HBsAg) "a" determinant affects the detection sensitivity of an HBsAg diagnostic kit

Dear editor:

Hepatitis B virus surface antigen (HBsAg) is one of the most important serological markers used in the diagnosis of HBV infection. HBV has been classified into 8 genotypes, designated A to H [1–4]. In our previous report [5], we evaluated the sensitivity of 10 commercially available diagnostic kits to recombinant HBsAgs encoded by HBV of genotypes A to H. None of the diagnostic kits examined failed to detect HBsAg of all the genotypes (A to H) at a concentration of 1.0 IU/ml. When the HBsAg samples were tested at a lower concentration (0.2 IU/ml), 9 out of 10 kits gave positive results, i.e. cut-off index (COI) ≥ 1.0, but 1 kit, Lumipulse II HBsAg, failed to give positive results for genotypes E and F. In this study, we compared the amino acid sequences of the HBsAg "a" determinant among HBV genotypes.

Amino acid-substituted HBsAgs, i.e., S140T, for genotypes E and F were synthesized as follows: the S genes of genotypes E and F were cloned into the eukaryotic expression vector pEF6/V5-His (Invitrogen Co., San Diego, CA), as previously described [5]. We constructed the amino acid-substituted HBsAg mutants, S140T, by inverse PCR of the whole plasmids with KOD-plus polymerase (Toyobo Co., Ltd., Osaka, Japan) following the thermal cycler protocol; denaturation for 2 min at 94 °C and 30 cycles of denaturation at 94 °C for 1 s, annealing at 55 °C for 30 s, and extension at 68 °C for 6 min 30 s. Primers for PCR of the plasmid of genotype E were as follows: forward eS140T-Fw409-430, 5′-ATGTTGCTGTACAAAACCTTCGG-3′; reverse eS140T-Rv408-389, 5′-GAGGGAAACATAGAGGTTCC-3′. Primers for genotype F plasmid were as follows: forward fS140T-Fw409-430, 5′-CTGTTGCTGTACCAAACCCTCGG-3′; reverse fS140T-Rv408-389, 5′-GAGGGAAACATAGAGGTTCC-3′. Underlined characters in these DNA sequences refer to codon S140T in the S protein and boldface characters indicate the substituted nucleotide that was T in the wild-type sequence. PCR products were separated by agarose gel electrophoresis and isolated with the MinElute Gel kit (Qiagen GmbH, Germany), circularized using the Blunting Kination Ligation kit (Takara Bio Inc., Ohtsu, Japan), and used to transform TOP 10 Chemically Competent *Escherchia coli* cells (Invitrogen). The entire S gene regions of the resulting plasmids were sequenced to confirm that they had the desired substitution and no other mutation (data not shown). The above kits were used according to the respective manufacturer's instructions.

Huh-7 cells grown in two 6-well culture plates (Invitrogen) were transiently transfected with each HBsAg plasmid as previously described [5]. After 3 days of culture, approximately 40 ml of culture supernatant was harvested and filtered through a membrane filter with pore size of 0.45 mm (Millex® Filter Unit; Millipore Co., Billerica, MA). The supernatants were concentrated with Amicon Ultra-15 K10 (Millipore Co.) to one-fifth of the volume. The concentration of each recombinant HBsAg sample was tentatively determined using (expressed in IU/ml) Architect HBsAg QT (Abbott Japan Co., Ltd., Chiba, Japan), which is the only quantitative assay kit approved in Japan. The samples were diluted to make 2-fold serial dilutions at concentrations of 1.6 IU/ml to 0.1 IU/ml with a multi-marker negative matrix (Accurum 810; BBI Co. Ltd., Boston, MA). The test samples were measured with 2 diagnostic kits – Lumipulse II HBsAg and Lumipulse Presto HBsAg (Fujirebio Co. Ltd., Tokyo, Japan) – according to the manufacturer's instructions and the results were expressed as the COI.

Comparison of the amino acid sequences of the HBsAg "a" determinant among HBV genotypes revealed that the amino acid at position 140 was T (threonine) in all genotypes except E and F but was S (serine) in genotypes E and F (Fig. 1A). We therefore synthesized amino acid-substituted HBsAgs, i.e., S140T, for genotypes E and F. As shown in Fig. 1B, S140T of both genotypes, E and F, tested positive, i.e., COI ≥ 1.0, by the Lumipulse II HBsAg kit even at a low concentration (0.1 IU/ml) of HBsAg. These results indicated that a single amino acid substitution in the HBsAg "a" determinant affects the sensitivity of the Lumipulse II HBsAg kit. In response to these results, Fujirebio Inc., the manufacturer of the Lumipulse II HBsAg kit, improved the sensitivity of the kit by optimizing it for the amounts of the two types of monoclonal antibody used. As shown in Fig. 1C, the improved kit, named Lumipulse Presto HBsAg, was able to detect a concentration of HBsAg as low as 0.1 IU/ml regardless of the substitution at amino acid 140.

In this report, we demonstrate that a single amino acid substitution affects the sensitivity of an in vitro diagnostic kit for HBsAg detection. This issue has been of wide concern because it was well documented that some diagnostic kits failed to detect particular mutant HBsAgs that have an amino acid substitution in the "a" determinant, such as a Gly/Arg mutation at amino acid 145, i.e., G145R [6–8]. Our study clearly verified the influence of amino acid substitution in the HBsAg "a" determinant on the detection capacity of a diagnostic kit by using the amino acid substitution technique.

The effect of an amino acid substitution on the sensitivity of diagnostic kits may not be restricted to detection kits for HBsAg. The phenomenon reported here should be borne in mind when using in vitro diagnostic kits not only for HBsAg but also for other analytes, such as HCV core Ag and HIV Ag. In fact, our recent study demonstrated that a single amino acid substitution within the HCV core antigen sequence reduced the sensitivity of a commonly used immunoassay [9].

In conclusion, we have verified that a particular amino acid residue in the HBsAg "a" determinant of a particular HBV genotype is critical for HBsAg detection sensitivity. Furthermore, it was demonstrated that optimization for the amounts of monoclonal antibodies improved the sensitivity of an HBsAg detection kit. These results indicate that caution should be exercised when detecting HBsAgs of various genotypes as well as mutant HBsAgs.

Acknowledgments

We thank Fujirebio Inc. who supplied the HBsAg kits and in performing the assays. This study was supported by Grants-in-Aid from the Ministry of Health, Labour, and Welfare, Japan.

0009-8981/$ – see front matter
doi:10.1016/j.cca.2009.12.020

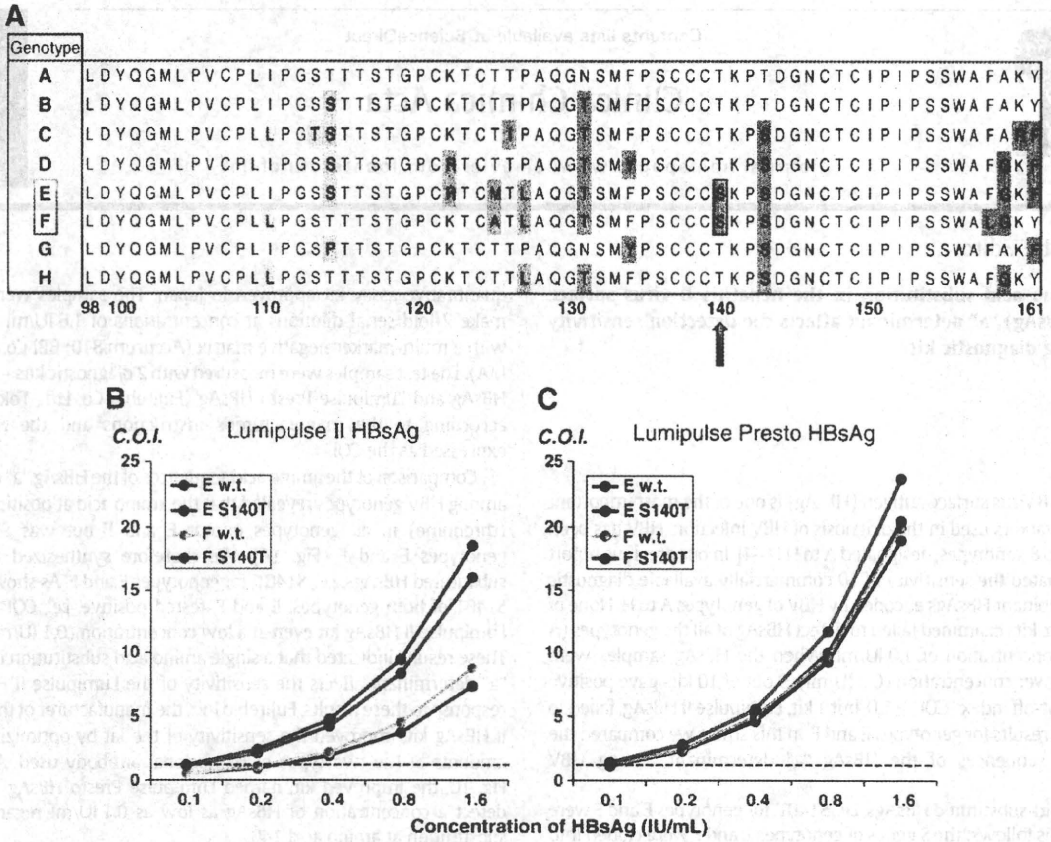

Fig. 1. A Comparison of amino acid sequences of HBsAg "a" determinants of various HBV genotypes. Accession numbers for amino acid sequences of genotypes A to H shown in the figure are listed below. Genotype A (AY902775, http://www.ncbi.nlm.nih.gov/nuccore/59802797); genotype B (AY293309, http://www.ncbi.nlm.nih.gov/nuccore/38147024); genotype C (AY205125, http://www.ncbi.nlm.nih.gov/nuccore/60279615); genotype D (AY796032, http://www.ncbi.nlm.nih.gov/nuccore/56090033); genotype E (DQ060829, http://www.ncbi.nlm.nih.gov/nuccore/70794948); genotype F (AY090459, http://www.ncbi.nlm.nih.gov/nuccore/22135721); genotype G (AB056516, http://www.ncbi.nlm.nih.gov/nuccore/15425700); genotype H (AB179747, http://www.ncbi.nlm.nih.gov/nuccore/60115422). B: Detection of recombinant HBsAg derived from genotypes E (E w.t.) and F (F w.t.) and their amino acid-substituted counterparts (E S140T and F S140T) by Lumipulse II HBsAg and C: Lumipulse Presto HBsAg kits. Each point indicates the mean of triplicate results. Error bars are too short to be indicated. Dashed lines indicate COI = 1.0.

References

[1] Arauz-Ruiz P, Norder H, Robertson BH, Magnius LO. Genotype H: a new Amerindian genotype of hepatitis B virus revealed in Central America. J Gen Virol 2002;83:2059–73.

[2] Norder H, Courouce AM, Magnius LO. Complete genomes, phylogenetic relatedness, and structural proteins of six strains of the hepatitis B virus, four of which represent two new genotypes. Virology 1994;198:489–503.

[3] Okamoto H, Tsuda F, Sakugawa H, et al. Typing hepatitis B virus by homology in nucleotide sequence: comparison of surface antigen subtypes. J Gen Virol 1988;69 (Pt 10):2575–83.

[4] Stuyver L, De Gendt S, Van Geyt C, et al. A new genotype of hepatitis B virus: complete genome and phylogenetic relatedness. J Gen Virol 2000;81:67–74.

[5] Mizuochi T, Okada Y, Umemori K, Mizusawa S, Yamaguchi K. Evaluation of 10 commercial diagnostic kits for in vitro expressed hepatitis B virus (HBV) surface antigens encoded by HBV of genotypes A to H. J Virol Methods 2006;136:254–6.

[6] Coleman PF, Chen YC, Mushahwar IK. Immunoassay detection of hepatitis B surface antigen mutants. J Med Virol 1999;59:19–24.

[7] Ly TD, Servant-Delmas A, Bagot S, et al. Sensitivities of four new commercial hepatitis B virus surface antigen (HBsAg) assays in detection of HBsAg mutant forms. J Clin Microbiol 2006;44:2321–6.

[8] Moerman B, Moons V, Sommer H, Schmitt Y, Stetter M. Evaluation of sensitivity for wild type and mutant forms of hepatitis B surface antigen by four commercial HBsAg assays. Clin Lab 2004;50:159–62.

[9] Mohsan S, Suzuki R, Kondo M, et al. Evaluation of hepatitis C virus core antigen assays in detecting recombinant viral antigens of various genotypes. J Clin Microbiol 2009;47:4141–3.

Toshiaki Mizuochi*
Saeko Mizusawa
Kiyoko Nojima
Yoshiaki Okada
Kazunari Yamaguchi
Department of Safety Research on Blood and Biological Products, National Institute of Infectious Diseases, 4-7-1, Gakuen Musashi-Murayama-shi, Tokyo 208-0011, Japan
*Corresponding author.
E-mail address: miz@nih.go.jp (T. Mizuochi).

13 October 2009

blood
2010 116: 4926-4933
Prepublished online Aug 23, 2010;
doi:10.1182/blood-2010-05-283358

Persistent expression of the full genome of hepatitis C virus in B cells induces spontaneous development of B-cell lymphomas in vivo

Yuri Kasama, Satoshi Sekiguchi, Makoto Saito, Kousuke Tanaka, Masaaki Satoh, Kazuhiko Kuwahara, Nobuo Sakaguchi, Motohiro Takeya, Yoichi Hiasa, Michinori Kohara and Kyoko Tsukiyama-Kohara

Blood (print ISSN 0006-4971, online ISSN 1528-0020), is published weekly by the American Society of Hematology, 2021 L St, NW, Suite 900, Washington DC 20036.

Persistent expression of the full genome of hepatitis C virus in B cells induces spontaneous development of B-cell lymphomas in vivo

*Yuri Kasama,[1] *Satoshi Sekiguchi,[2] Makoto Saito,[1] Kousuke Tanaka,[1] Masaaki Satoh,[1] Kazuhiko Kuwahara,[3] Nobuo Sakaguchi,[3] Motohiro Takeya,[4] Yoichi Hiasa,[5] Michinori Kohara,[2] and Kyoko Tsukiyama-Kohara[1]

[1]Department of Experimental Phylaxiology, Faculty of Life Sciences, Kumamoto University, Kumamoto, Japan; [2]Department of Microbiology and Cell Biology, Tokyo Metropolitan Institute of Medical Science, Tokyo, Japan; [3]Department of Immunology, Faculty of Life Sciences, Kumamoto University, Kumamoto, Japan; [4]Department of Cell Pathology, Faculty of Life Sciences, Kumamoto University, Kumamoto, Japan; and [5]Department of Gastroenterology and Metabology, Ehime University Graduate School of Medicine, To-on, Ehime, Japan

Extrahepatic manifestations of hepatitis C virus (HCV) infection occur in 40%-70% of HCV-infected patients. B-cell non-Hodgkin lymphoma is a typical extrahepatic manifestation frequently associated with HCV infection. The mechanism by which HCV infection of B cells leads to lymphoma remains unclear. Here we established HCV transgenic mice that express the full HCV genome in B cells (RzCD19Cre mice) and observed a 25.0% incidence of diffuse large B-cell non-Hodgkin lymphomas (22.2% in males and 29.6% in females) within 600 days after birth. Expression levels of aspartate aminotransferase and alanine aminotransferase, as well as 32 different cytokines, chemokines and growth factors, were examined. The incidence of B-cell lymphoma was significantly correlated with only the level of soluble interleukin-2 receptor α subunit (sIL-2Rα) in RzCD19Cre mouse serum. All RzCD19Cre mice with substantially elevated serum sIL-2Rα levels (> 1000 pg/mL) developed B-cell lymphomas. Moreover, compared with tissues from control animals, the B-cell lymphoma tissues of RzCD19Cre mice expressed significantly higher levels of IL-2Rα. We show that the expression of HCV in B cells promotes non-Hodgkin–type diffuse B-cell lymphoma, and therefore, the RzCD19Cre mouse is a powerful model to study the mechanisms related to the development of HCV-associated B-cell lymphoma. (*Blood*. 2010;116(23):4926-4933)

Introduction

More than 175 million people worldwide are infected with hepatitis C virus (HCV), a positive-strand RNA virus that infects both hepatocytes and peripheral blood mononuclear cells.[1] Chronic HCV infection may lead to hepatitis, liver cirrhosis, hepatocellular carcinomas[2,3] and lymphoproliferative diseases such as B-cell non-Hodgkin lymphoma and mixed-cryoglobulinemia.[1,4-6] B-cell non-Hodgkin lymphoma is a typical extrahepatic manifestation frequently associated with HCV infection[7] with geographic and ethnic variability.[8,9] Based on a meta-analysis, the prevalence of HCV infection in patients with B-cell non-Hodgkin lymphoma is approximately 15%.[8] The HCV envelope protein E2 binds human CD81,[10] a tetraspanin expressed on various cell types including lymphocytes, and activates B-cell proliferation[11]; however, the precise mechanism of disease onset remains unclear. We previously developed a transgenic mouse model that conditionally expresses HCV cDNA (nucleotides 294-3435), including the viral genes that encode the core, E1, E2, and NS2 proteins, using the Cre/*lox*P system (in core~NS2 [CN2] mice).[12,13] The conditional transgene activation of the HCV cDNA (core, E1, E2, and NS2) protects mice from Fas-mediated lethal acute liver failure by inhibiting cytochrome c release from mitochondria.[13] In HCV-infected mice, persistent HCV protein expression is established by targeted disruption of *irf-1*, and high incidences of lymphoproliferative disorders are found in CN2 *irf-1*$^{-/-}$ mice.[14] Infection and replication of HCV also occur in B cells,[15,16] although the direct effects, particularly in vivo, of HCV infection on B cells have not been clarified.

To define the direct effect of HCV infection on B cells in vivo, we crossed transgenic mice with an integrated full-length HCV genome (Rz) under the conditional Cre/*lox*P expression system with mice expressing the Cre enzyme under transcriptional control of the B lineage–restricted gene *CD19*,[17] we addressed the effects of HCV transgene expression in this study.

Methods

Animal experiments

Wild-type (WT), Rz, CD19Cre, RzCD19Cre mice (129/sv, BALB/c, and C57BL/6J mixed background), and MxCre/CN2-29 mice (C57BL/6J background) were maintained in conventional animal housing under specific pathogen-free conditions. All animal experiments were performed according to the guidelines of the Tokyo Metropolitan Institute of Medical Science or the Kumamoto University Subcommittee for Laboratory Animal Care. The protocol was approved by the Institutional Review Boards of both facilities.

Measurements of HCV protein and RNA

Mice were anesthetized and bled, and tissues (spleen, lymph nodes, liver, and tumors) were homogenized in lysis buffer (1% sodium dodecyl sulfate; 0.5% (wt/vol) nonyl phenoxypolyethoxylethanol; 0.15M NaCl; 10 mM

Submitted May 2, 2010; accepted August 13, 2010. Prepublished online as *Blood* First Edition paper, August 23, 2010; DOI 10.1182/blood-2010-05-283358.

*Y.K. and S.S. contributed equally to this work.

The online version of this article contains a data supplement.

The publication costs of this article were defrayed in part by page charge payment. Therefore, and solely to indicate this fact, this article is hereby marked "advertisement" in accordance with 18 USC section 1734.

tris(hydroxymethyl)aminomethane, pH 7.4) using a Dounce homogenizer. The concentration of HCV core protein in tissue lysates was measured using an HCV antigen enzyme-linked immunosorbent assay (ELISA; Ortho).[18] HCV mRNA was isolated by a guanidine thiocyanate protocol using ISOGEN (Nippon Gene) and was detected by reverse transcription polymerase chain reaction (RT-PCR) amplification using primers specific for the 5′ untranslated region of the *HCR6* sequence.[19,20] Reverse transcription was performed using Superscript III reverse transcriptase (Invitrogen) with random primers. PCR primers NCR-F (5′-TTCACGCAGAAAGCGTCTAGCCAT-3′) and NCR-R (5′-TCGTCCTGGCAATTCCGGTGTACT-3′) were used for the first round of HCV cDNA amplification, and the resulting product was used as a template for a second round of amplification using primers NCR-F INNER (5′-TTCCGCAGACCACTATGGCT-3′) and NCR-R INNER (5′-TTCCGCAGACCACTATGGCT-3′).

Collection of serum for chemokine ELISA

Blood samples were collected from the supraorbital veins or by heart puncture of killed mice. Blood samples were centrifuged at 10 000*g* for 15 minutes at 4°C to isolate the serum.[21] Serum concentrations of interleukin (IL)–1α, IL-1β, IL-2, IL-3, IL-4, IL-5, IL-6, IL-9, IL-10, IL-12(p40), IL-12(p70), IL-13, IL-17, Eotaxin, granulocyte colony-stimulating factor (CSF), granulocyte–macrophage–CSF, interferon (IFN)–γ, keratinocyte-derived chemokine (KC), monocyte chemotactic protein-1, macrophage inflammatory protein (MIP)–1α, MIP-1β, Regulated upon Activation, Normal T-cell Expressed, and Secreted, tumor necrosis factor-α, IL-15, fibroblast growth factor-basic, leukemia inhibitory factor, macrophage-CSF, human monokine induced by gamma interferon, MIP-2, platelet-derived growth factorβ, and vascular endothelial growth factor were measured using the Bio-Plex Pro assay (Bio-Rad). Serum soluble IL-2 receptor α (sIL-2Rα) concentrations were determined by ELISA (DuoSet ELISA Development System; R&D Systems). Serum aspartate aminotransferase (AST) and alanine aminotransferase (ALT) activities were determined using a commercially available kit (Transaminase CII test; Wako Pure Chemical Industries).

Histology and immunohistochemical staining

Mouse tissues were fixed with 4% formaldehyde (Mildform 10 N; Wako Pure Chemical Industries), dehydrated with an ethanol series, embedded in paraffin, sectioned (10-μm thick) and stained with hematoxylin and eosin. For tissue immunostaining, paraffin was removed from the sections using xylene following the standard method,[14] and sections were incubated with anti-CD3 or anti-CD45R (Santa Cruz Biotechnology) in phosphate-buffered saline without Ca^{2+} and Mg^{2+} (pH 7.4) but with 5% skim milk. Next, the sections were incubated with biotinylated anti-rat immunoglobulin (Ig)G (1:500), followed by incubation with horseradish peroxidase-conjugated avidin-biotin complex (Dako Corp), and the color reaction was developed using 3,3′-diaminobenzidine. Sections were observed under an optical microscope (Carl Zeiss).

Detection of immunoglobulin gene rearrangements by PCR

Genomic DNA was isolated from tumor tissues, and PCR was performed as described.[22] In brief, PCR reaction conditions were 98°C for 3 minutes; 30 cycles at 98°C for 30 seconds, 60°C for 30 seconds, 72°C for 1.5 minutes, and 72°C for 10 minutes. Mouse Vk genes were amplified using previously described primers.[23] Amplification of mouse Vj genes was performed using Vκcon (5′-GGCTGCAGSTTCAGTGGCAGTGGRTCWGGRAC-3′; R, purine; W, A or T) and Jκ5 (5′-TGCCACGTCAACTGATAATGAGCCCTCTC-3′) as described.[24]

Results

Establishment of transgenic mice with B lineage–restricted HCV gene expression

We defined the direct effect of HCV infection on B cells in vivo by crossing transgenic mice that had an integrated full-length HCV genome (Rz) under the conditional Cre/*lox*P expression system (Figure 1A upper schematic)[12,19,25] with mice that expressed the Cre enzyme under transcriptional control of the B lineage–restricted gene *CD19*[17] (RzCD19Cre; Figure 1A lower schematic). Expression of the HCV transgene in RzCD19Cre mice was confirmed by ELISA (Figure 1B); a substantial level of HCV core protein was detected in the spleen (370.9 ± 10.2 pg/mg total protein), but levels were lower in the liver (0.32 ± 0.03 pg/mg) and plasma (not detectable). RT-PCR analysis of peripheral blood lymphocytes (PBLs) from RzCD19Cre mice indicated the presence of HCV transcripts (Figure 1C). The weights of RzCD19Cre, Rz (with the full HCV genome transgene alone), CD19Cre (with the Cre gene knock-in at the CD19 gene locus) and WT mice were measured weekly for more than 600 days post birth; there were no significant differences between these groups (data not shown; the total number of transgenic and WT mice was approximately 200). The survival rate in each group was also measured for > 600 days (Figure 1D); survival in the female RzCD19Cre group was lower than that of the other groups.

The spontaneous development of B-cell lymphomas in the RzCD19Cre mouse

At 600 days post birth, mice (n = 140) were killed by bleeding under anesthesia, and tissues (spleen, lymph node, liver, and tumors) were excised and examined by hematoxylin and eosin staining (Figure 2A; supplemental Figure 1, available on the *Blood* Web site; see the Supplemental Materials link at the top of the online article). The incidence of B-cell lymphoma in RzCD19Cre mice was 25.0% (22.2% in males and 29.6% in females) and was significantly higher than the incidence in the HCV-negative groups (Table 1). This incidence is significantly higher than those of the other cell-type tumors developed spontaneously in all mouse groups (supplemental Table 1). Because nodular proliferation of CD45R-positive atypical lymphocytes was observed, lymphomas were diagnosed as typical diffuse B-cell non-Hodgkin lymphomas (Figure 2Aiv,vi-vii; supplemental Figure 1B,E,H,M). Mitotic cells were also positive for CD45R (Figure 2Avi arrowheads). CD3-positive T-lymphocytes were small and had a scattered distribution. Intrahepatic lymphomas had the same immunophenotypic characteristics as B-cell lymphomas (supplemental Figure 1K arrowheads, inset; 1L–N, ID No. 24-4, RzCD19Cre mouse); lymphoma tissues were markedly different compared with the control lymph node (Figure 2Ai,iii,v; ID No. 47-4, CD19Cre mouse) and liver (supplemental Figure 1J; ID No. 24-2, Rz mouse; tissues were from a littermate of the mice used to generate the data in supplemental Figure 1D-I,K-N). All samples were reviewed by at least 2 expert pathologists and classified according to World Health Organization classification.[26] Lymphomas were mostly CD45R positive and located in the mesenteric lymph nodes (Figure 2A; supplemental Figure 1), and some were identified as intrahepatic lymphomas (incidence, 4.2%; supplemental Figure 1K-N). HCV gene expression was detected in all B-cell lymphomas of RzCD19Cre mice (Figure 2B).

To examine the Ig gene configuration in the B-cell lymphomas of the RzCD19Cre mice, genomic DNA was isolated and analyzed by PCR. Ig gene rearrangements were identified in each case (Figure 2C). Genomic DNA isolated from the tumors of a germinal center–associated nuclear protein (GANP) transgenic mouse (GANP Tg#3) yielded a predominant Jk5 PCR product (Figure 2C, Vκ-Jκ); a predominant JH1 product and a minor JH2 product (supplemental Figure 2, DH-JH) were also identified, as previously reported,[22] indicating that the lymphoma cells proliferated from the transformation of an oligo B-cell clone. The B-cell lymphomas of

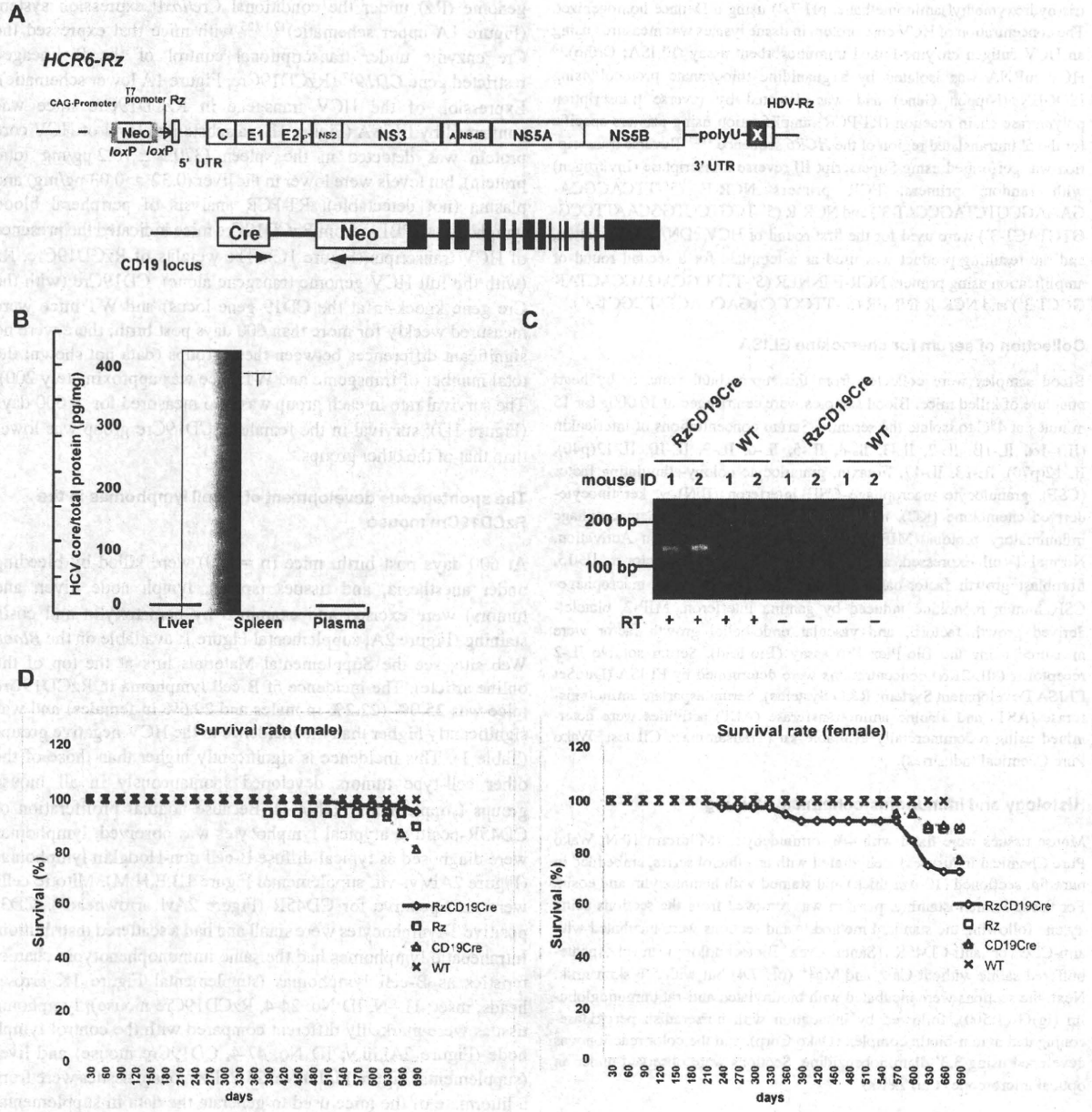

Figure 1. Establishment of RzCD19Cre mice. (A) Schematic diagram of the transgene structure comprising the complete HCV genome (*HCR6-Rz*). HCV genome expression was regulated by the Cre/*lox*P expression cassette (top diagram). The Cre transgene was located in the CD19 locus (bottom diagram). (B) Expression of HCV core protein in the liver, spleen, and plasma of RzCD19Cre mice was quantified by core ELISA. Data represent the mean ± SD (n = 3). (C) Detection of HCV RNA in PBLs by RT-PCR. Samples that included the RT reaction are indicated by +, and those that did not include the RT reaction are indicated by –. (D) Survival rates of male and female RzCD19Cre mice (males, n = 45; females, n = 40), Rz mice (males, n = 20; females, n = 19), CD19Cre mice (males, n = 16; females, n = 22), and WT mice (males, n = 5; females, n = 10).

8 RzCD19Cre mice (mouse ID Nos. 24-1, 54-1, 56-5, 69-5, 42-4, 43-4, 36-3 [data not shown] and 62-2 [data not shown]) yielded a Jκ-5 gene amplification product, and the lymphomas from 3 other mice had the alternative gene configurations Jκ-1 (mouse ID No. 31-4), Jκ-2 (mouse ID No. 24-4) and Jκ-3 (mouse ID No. 42-4; Figure 2C). PCR amplification products from the genes JH4 (mouse ID Nos. 24-1, 24-4, 54-1, 43-4, 56-5, 69-5, 62-2 [data not shown], 36-3 [data not shown]), JH1 (mouse ID Nos. 31-4, 42-4) and JH3 (mouse ID Nos. 31-4, 42-4, 56-5, 43-4, 36-3 [data not shown]) were also detected (supplemental Figure 2). The mutation frequencies in the Jκ-1, -3 and -5 genes were the same as the mutation frequency in the genomic V-region gene.[22] Few or no sequence differences in the variable region were identified among clones from which DNA was amplified. These results indicate the possibility that tumors judged as B-cell lymphomas based on pathology criteria were derived from the transformation of a single germinal center of B-cell origin.

To rule out the oncogenic effect caused by a transgenic integration into a specific genomic locus, we examined if HCV transgene inserted into another genomic site also causes B-cell lymphomas using another HCV transgenic mouse strain, MxCre/CN2-29 (supplemental Figure 3). Expression of the HCV CN2

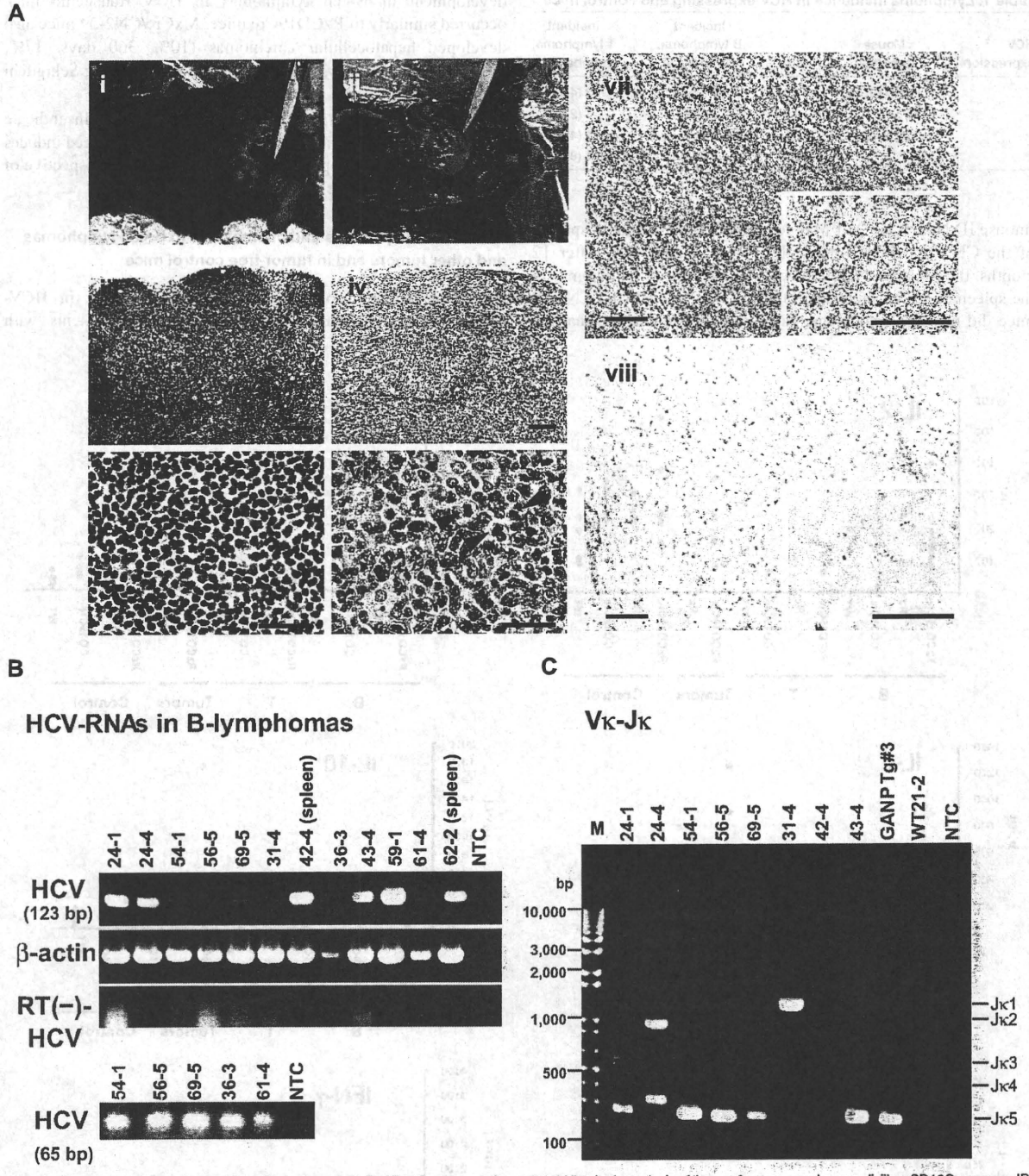

Figure 2. Histopathologic analysis of B-cell lymphomas in RzCD19Cre mouse tissues. (A) Histologic analysis of tissues from a normal mouse (i, iii, v; CD19Cre mouse, ID No. 47-4, male) and a B-cell lymphoma from a RzCD19Cre mouse (ii, iv, vi; ID No. 69-5, male). Paraformaldehyde-fixed and paraffin-embedded tumor tissues were stained with hematoxylin and eosin (iii-vi) or immunostained using anti-CD45R (vii; bottom right, inset) and anti-CD3 (viii; bottom right, inset). Also shown is a macroscopic view of the lymphoma from a mesenchymal lymph node (ii, indicated by forceps), which is not visible in the normal mouse (i). Mitotic cells are indicated with arrowheads (vi). Scale bars: 100 μm (iii-iv, vii-viii) and 20 μm (v-vi, insets in vii-viii). (B) Expression of HCV RNA in B-cell lymphomas from RzCD19Cre mice was examined by RT-PCR. The first round of PCR amplification yielded a 123-base pair fragment of HCV cDNA (upper panel), and a second round of PCR amplification yielded a 65-base pair fragment (lower panel). The β-actin mRNA was a control. As an additional control, the first and second rounds of amplification were performed using samples that had not been subjected to reverse transcription. NTC, no-template control. (C) Ig gene rearrangements in the tumors of RzCD19Cre mice. Genomic DNA isolated from B-cell lymphoma tissues of RzCD19Cre mice (ID Nos. 24-1, 24-4, 54-1, 56-5, 69-5, 31-4, 42-4, 43-4) and spleen tissues of a WT mouse (ID No. 21-2) was PCR amplified using primers specific for Vκ-Jκ genes. Amplification of controls was performed using genomic DNA isolated from a GANP transgenic mouse (GANP Tg#3) and in the absence of template DNA (no-template control, NTC). M, DNA ladder marker.

gene (nucleotides 294-3435)[12] was induced by the Mx promoter-driven cre recombinase with poly(I:C) induction[14] (supplemental Figure 3A). HCV core proteins were detected in both normal spleen (mouse ID Nos. 2, 3, 4) and intra-splenic B-cell lymphoma tissues

Table 1. Lymphoma incidence in HCV-expressing and control mice

HCV expression	Mouse genotype	No.	Incident B lymphoma, number (%)	Incident T lymphoma, number (%)
+	RzCD19Cre	72	18 (25.0)	3 (4.1)
–	Rz	34	1 (2.9)	1 (2.9)
–	CD19Cre	22	2 (9.1)	1 (4.5)
–	WT	12	1 (8.3)	1 (8.3)

(mouse ID Nos. 5, 6, 7) of MxCre/CN2-29 mice but not in spleens of the CN2-29 mouse (mouse ID No. 1, Figure 3B). After 12 months, the MxCre/CN2-29 mice developed B-cell lymphomas in the spleen at a high incidence (33.3%: 3/9), whereas the CN2-29 mice did not (0/13; supplemental Figure 3C), indicating that the development of B-cell lymphomas in HCV transgenic mice occurred similarly to RzCD19Cre mice. MxCre/CN2-29 mice also developed hepatocellular carcinomas (10%, 360 days, 17%, 480 days, 50%, 600 days after onset of HCV expression; Sekiguchi et al, submitted).

The results obtained in 2 HCV transgenic mouse strains indicate that the expression of the HCV gene or the proteins indeed induces the spontaneous development of B-cell lymphomas irrespective of the integrated site in the mouse genome.

The levels of cytokines and chemokines in B-cell lymphomas and other tumors and in tumor-free control mice

Abnormal induction of cytokine production occurs in HCV-associated non-Hodgkin lymphomas[27,28] and in patients with

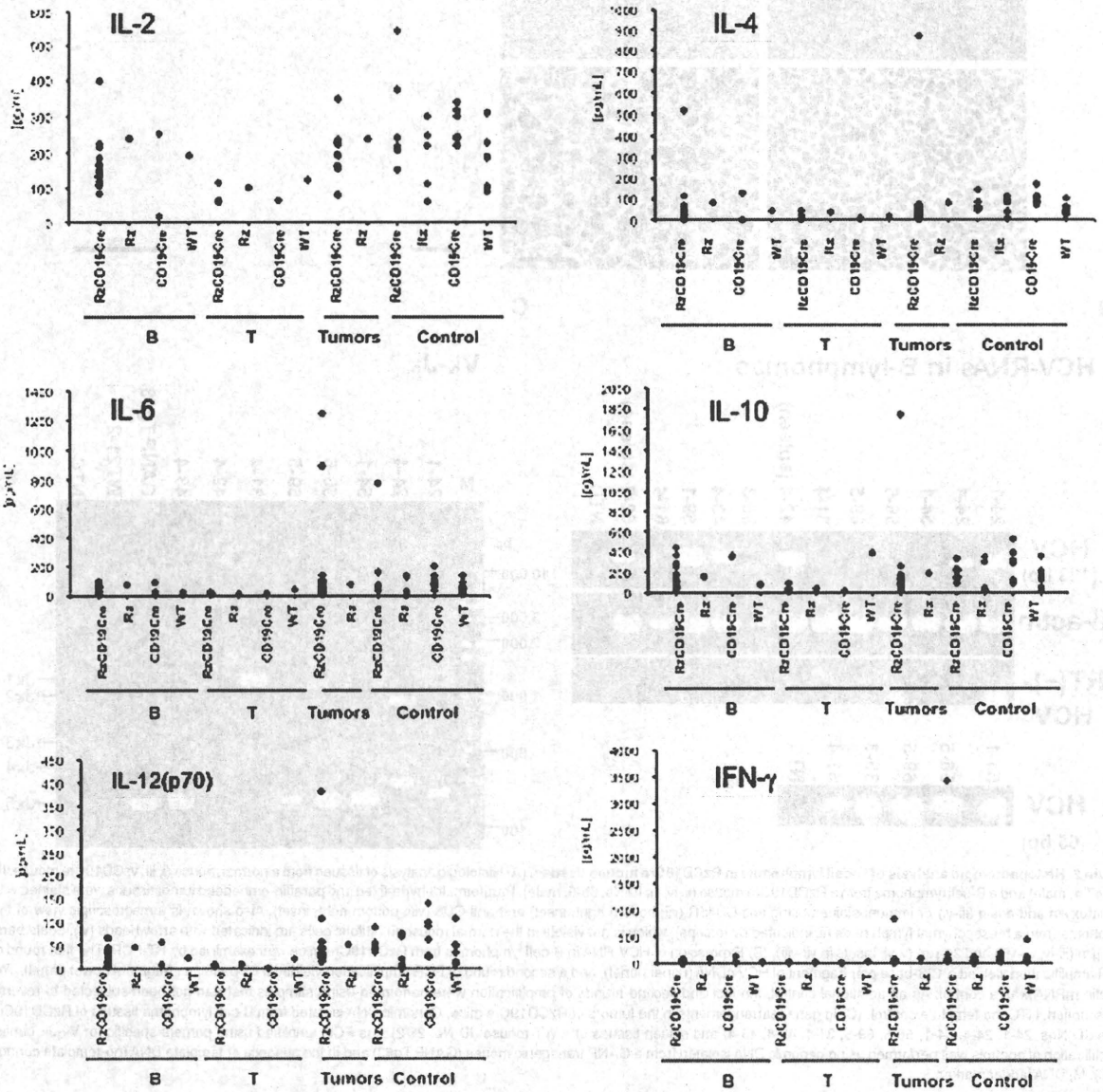

Figure 3. Analysis of serum cytokine levels using a multisuspension array system. The serum concentration levels of IL-2, IL-4, IL-6, IL-10, IL-12(p70), and IFN-γ were measured in RzCD19Cre mice with B-cell lymphomas (B), T-cell lymphomas (T), and other tumors (mammary tumor, sarcoma, and hepatocellular carcinoma) and in tumor-free RzCD19Cre, Rz, CD19Cr,e and WT mice.

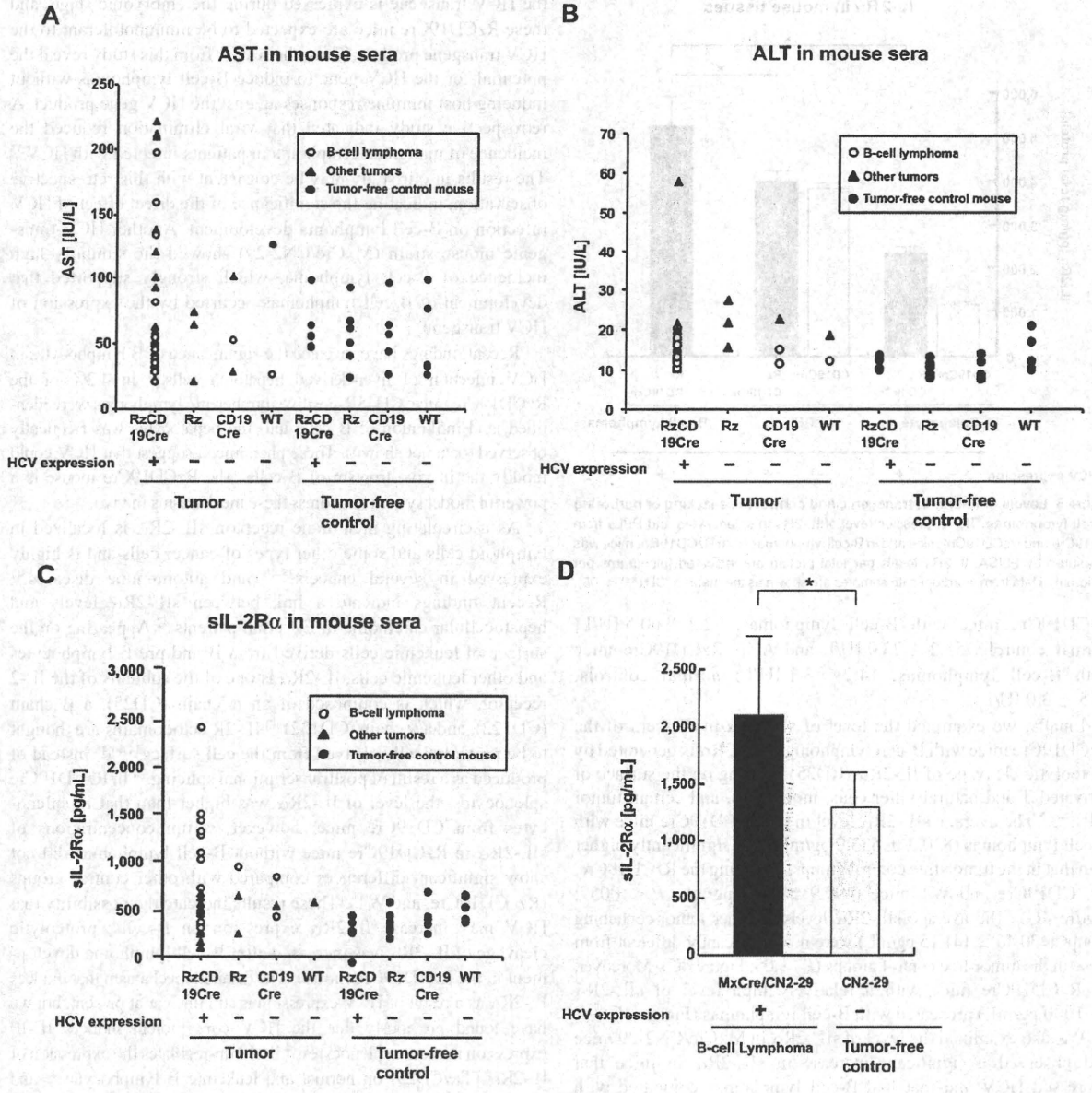

Figure 4. Serum titers of AST, ALT and soluble IL-2Rα in transgenic and control mice lacking or harboring B-cell lymphomas. (A-B) The AST (A) and ALT (B) assays were performed on serum samples from tumor-free control mice and the RzCD19Cre, Rz, CD19Cre and WT mice with or without B-cell lymphomas or other tumors. (C) ELISA analysis was performed to determine the sIL-2Rα concentration in serum samples from tumor-free control mice and the RzCD19Cre, Rz, CD19Cre, and WT mice with or without B-cell lymphomas or other tumors. (D) Concentration of soluble IL-2Rα in sera from transgenic (MxCre/CN2-29 or CN2-29) mice with or without B-cell lymphomas (*$P < .05$).

chronic hepatitis.[29,30] Therefore, we examined tumor cytokine and chemokine levels using a multisuspension array system. The levels of IL-2, IL-4, IL-6, IL-10, IL-12(p70), and IFN-γ (Figure 3), which may have a link with lymphoproliferation[14] or lymphoma[28,31] induced by HCV, and IL-1α, IL-1β, IL-3, IL-5, IL-9, IL-12(p40), IL-13, IL-17, Eotaxin, granulocyte-CSF, granulocyte–macrophage–CSF, KC, monocyte chemotactic protein-1, MIP-1α, MIP-1β, Regulated upon Activation, Normal T-cell Expressed, and Secreted, tumor necrosis factor-α, IL-15, fibroblast growth factor-basic, leukemia inhibitory factor, macrophage-CSF, human monokine induced by gamma interferon, MIP-2, platelet-derived growth factorβ and vascular endothelial growth factor (supplemental Figure 4) were measured in sera from mice with B-cell lymphomas, T-cell lymphomas, and other tumors and in sera from tumor-free RzCD19Cre, Rz, CD19Cre, and WT control mice. The levels of these cytokines and chemokines in sera from tumor-bearing RzCD19Cre mice with B-cell lymphomas were not significantly different from those of the control groups, and thus, changes in the expression of these cytokines and chemokines were not strictly correlated with the occurrence of B-cell lymphoma in RzCD19Cre mice.

The levels of amino transferases and sIL-2Rα in mice lacking or harboring B-cell lymphomas

We also examined the levels of AST and ALT in the RzCD19Cre, Rz, CD19Cre, and WT mice. There were no significant differences in the levels of AST and ALT in the sera of mice lacking or harboring B-cell lymphomas ($P > .05$; Figure 4A-B; AST:

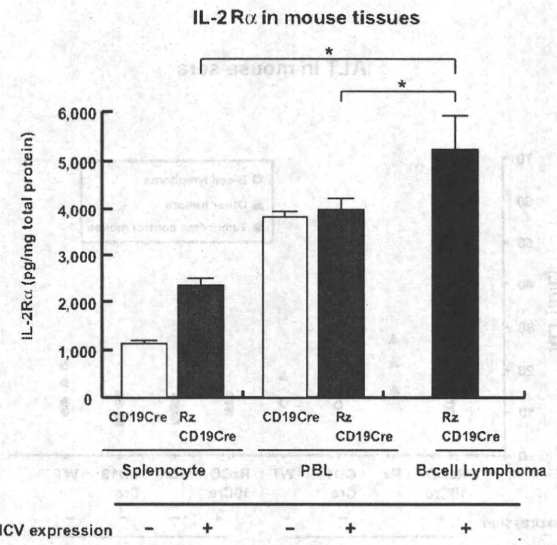

Figure 5. Levels of IL-2Rα in transgenic and control mice lacking or harboring B-cell lymphomas. The expression level of IL-2Rα in splenocytes and PBLs from CD19Cre and RzCD19Cre mice and in B-cell lymphomas from RzCD19Cre mice was measured by ELISA. IL-2Rα levels per total protein are indicated (picograms per milligram). Data from quadruplicate samples are shown as the mean ± SD (*$P < .05$).

RzCD19Cre mice with B-cell lymphomas, 72.2 ± 60.5 IU/L; normal controls, 55.2 ± 23.0 IU/L and ALT: RzCD19Cre mice with B-cell lymphomas, 14.2 ± 3.1 IU/L; normal controls, 11.5 ± 3.0 IU/L).

Finally, we examined the level of sIL-2Rα in the sera of the RzCD19Cre mice with B-cell lymphomas; sIL-2Rα is generated by proteolytic cleavage of IL-2Rα (CD25) residing on the surface of activated T and natural killer cells, monocytes, and certain tumor cells.[24,32] The average sIL-2Rα level in the RzCD19Cre mice with B-cell lymphomas (830.3 ± 533.0 pg/mL) was significantly higher than that in the tumor-free control groups, including the RzCD19Cre, Rz, CD19Cre and WT mice (499.9 ± 110.2 pg/mL; $P < .0057$; Figure 4C). The average sIL-2Rα levels in other tumor-containing groups (430.46 ± 141.15 pg/mL) were not significantly different from those in the tumor-free control groups ($P > .05$; Figure 4C). Moreover, all RzCD19Cre mice with a relatively high level of sIL-2Rα (> 1000 pg/mL) presented with B-cell lymphomas (Figure 4C).

We also examined the level of sIL-2Rα in MxCre/CN2-29 mice and observed a significant increase in sIL-2Rα in mice that expressed HCV and that had B-cell lymphomas compared with tumor-free control (CN2-29) mice (Figure 4D).

Expression of IL-2Rα in B-cell lymphomas of the RzCD19Cre mice

To examine whether sIL-2Rα was derived from lymphoma tissues, we quantified IL-2Rα concentrations in splenocytes, PBLs and B-cell lymphoma tissues (Figure 5). The concentration of IL-2Rα was significantly higher in splenocytes from RzCD19Cre mice compared with those from CD19Cre mice; the concentration was even higher in B-cell lymphoma tissues than in splenocytes from RzCD19Cre mice (Figure 5). These results strongly suggest that B-cell lymphomas directly contribute to the elevated serum concentrations of sIL-2Rα in RzCD19Cre mice.

Discussion

We have established HCV transgenic mice that have a high incidence of spontaneous B-cell lymphomas. In this animal model, the HCV transgene is expressed during the embryonic stage, and these RzCD19Cre mice are expected to be immunotolerant to the HCV transgene product. Thus, the results from this study reveal the potential for the HCV gene to induce B-cell lymphomas without inducing host immune responses against the HCV gene product. A retrospective study indicated that viral elimination reduced the incidence of malignant lymphoma in patients infected with HCV.[33] The results in our study may be consistent with this retrospective observation, indicating the significance of the direct effect of HCV infection on B-cell lymphoma development. Another HCV transgenic mouse strain (MxCre/CN2-29) showed the similarly high incidence of B-cell lymphoma, which strongly supported that development of B-cell lymphomas occurred by the expression of HCV transgene.

Recent findings have revealed the significance of B lymphocytes in HCV infection of liver-derived hepatoma cells.[34] In 4.2% of the RzCD19Cre mice, CD45R-positive intrahepatic lymphomas were identified, and infiltration of B cells into the hepatocytes was frequently observed (data not shown). These phenomena suggest that HCV could modify the in vivo tropism of B cells. The RzCD19Cre mouse is a powerful model system to address these mechanisms in vivo.

As a circulating membrane receptor, sIL-2Rα is localized in lymphoid cells and some other types of cancer cells and is highly expressed in several cancers[35-40] and autoimmune diseases.[41] Recent findings indicate a link between sIL-2Rα levels and hepatocellular carcinoma in Egyptian patients.[42] Appearing on the surface of leukemic cells derived from B and pre-B lymphocytes and other leukemic cells, IL-2Rα is one of the subunits of the IL-2 receptor, which is composed of an α chain (CD25), a β chain (CD122), and a γ chain (CD132).[43] IL-2R ectodomains are thought to be proteolytically cleaved from the cell surface[34,44,45] instead of produced as a result of posttranscriptional splicing.[24] In RzCD19Cre splenocytes, the level of IL-2Rα was higher than that in splenocytes from CD19Cre mice; however, serum concentrations of sIL-2Rα in RzCD19Cre mice without B-cell lymphomas did not show significant differences compared with other control groups (Rz, CD19Cre, and WT). These results indicate the possibility that HCV may increase IL-2Rα expression on B-cells; proteolytic cleavage of IL-2Rα was increased after B-cell lymphoma development in the RzCD19Cre mouse. The detailed mechanism that induces IL-2Rα as a result of HCV expression is still unclear at present, but we have found previously that the HCV core protein induces IL-10 expression in mouse splenocytes.[14] IL-10 up-regulates the expression of IL-2Rα (Tac/CD25) on normal and leukemic B lymphocytes,[46] and therefore, through IL-10, the HCV core protein might induce IL-2Rα in B cells of the RzCD19Cre mouse.

In conclusion, this study established an animal model that will likely provide critical information for the elucidation of molecular mechanism(s) underlying the spontaneous development of B-cell non-Hodgkin lymphoma after HCV infection. This knowledge should lead to therapeutic strategies to prevent the onset and/or progression of B-cell lymphomas.

Acknowledgments

We thank Dr T. Ito for assistance with pathology characterization and Dr T. Munakata for valuable comments.

This work was supported by grants from the Ministry of Health and Welfare of Japan and the Cooperative Research Project on Clinical and Epidemiologic Studies of Emerging and Re-emerging Infectious Diseases.

Authorship

Contribution: K.T.-K. conceived of the project; K.K., M.K., and K.T.-K. designed the studies; Y.K., S.S., M. Saito, K.T., M. Satoh, M.T., and K.T.-K. performed experiments and analyses; N.S. and Y.H. provided scientific advice; and K.T.-K. wrote the manuscript.

Conflict-of-interest disclosure: The authors declare no competing financial interests.

Correspondence: Kyoko Tsukiyama-Kohara, Department of Experimental Phylaxiology, Faculty of Life Sciences, Kumamoto University, Kumamoto 860-8556, Japan; e-mail: kkohara@kumamoto-u.ac.jp.

References

1. Ferri C, Monti M, La Civita L, et al. Infection of peripheral blood mononuclear cells by hepatitis C virus in mixed cryoglobulinemia. *Blood.* 1993; 82(12):3701-3704.
2. Saito I, Miyamura T, Ohbayashi A, et al. Hepatitis C virus infection is associated with the development of hepatocellular carcinoma. *Proc Natl Acad Sci U S A.* 1990;87(17):6547-6549.
3. Simonetti RG, Camma C, Fiorello F, et al. Hepatitis C virus infection as a risk factor for hepatocellular carcinoma in patients with cirrhosis. A case-control study. *Ann Intern Med.* 1992;116(2):97-102.
4. Silvestri F, Pipan C, Barillari G, et al. Prevalence of hepatitis C virus infection in patients with lymphoproliferative disorders. *Blood.* 1996;87(10): 4296-4301.
5. Ascoli V, Lo Coco F, Artini M, Levrero M, Martelli M, Negro F. Extranodal lymphomas associated with hepatitis C virus infection. *Am J Clin Pathol.* 1998;109(5):600-609.
6. Mele A, Pulsoni A, Bianco E, et al. Hepatitis C virus and B-cell non-Hodgkin lymphomas: an Italian multicenter case-control study. *Blood.* 2003; 102(3):996-999.
7. Dammacco F, Sansonno D, Piccoli C, Racanelli V, D'Amore FP, Lauletta G. The lymphoid system in hepatitis C virus infection: autoimmunity, mixed cryoglobulinemia, and overt B-cell malignancy. *Semin Liver Dis.* 2000;20(2):143-157.
8. Gisbert JP, Garcia-Buey L, Pajares JM, Moreno-Otero R. Prevalence of hepatitis C virus infection in B-cell non-Hodgkin's lymphoma: systematic review and meta-analysis. *Gastroenterology.* 2003;125(6):1723-1732.
9. Negri E, Little D, Boiocchi M, La Vecchia C, Franceschi S. B-cell non-Hodgkin's lymphoma and hepatitis C virus infection: a systematic review. *Int J Cancer.* 2004;111(1):1-8.
10. Pileri P, Uematsu Y, Campagnoli S, et al. Binding of hepatitis C virus to CD81. *Science.* 1998; 282(5390):938-941.
11. Rosa D, Saletti G, De Gregorio E, et al. Activation of naive B lymphocytes via CD81, a pathogenetic mechanism for hepatitis C virus-associated B lymphocyte disorders. *Proc Natl Acad Sci U S A.* 2005;102(51):18544-18549.
12. Wakita T, Taya C, Katsume A, et al. Efficient conditional transgene expression in hepatitis C virus cDNA transgenic mice mediated by the Cre/loxP system. *J Biol Chem.* 1998;273(15):9001-9006.
13. Machida K, Tsukiyama-Kohara K, Seike E, et al. Inhibition of cytochrome c release in Fas-mediated signaling pathway in transgenic mice induced to express hepatitis C viral proteins. *J Biol Chem.* 2001;276(15):12140-12146.
14. Machida K, Tsukiyama-Kohara K, Sekiguch S, et al. Hepatitis C virus and disrupted interferon signaling promote lymphoproliferation via type II CD95 and interleukins. *Gastroenterology.* 2009; 137(1):285-296,296 e281-211.
15. Lerat H, Rumin S, Habersetzer F, et al. In vivo tropism of hepatitis C virus genomic sequences in hematopoietic cells: influence of viral load, viral genotype, and cell phenotype. *Blood.* 1998; 91(10):3841-3849.
16. Karavattathayyil SJ, Kalkeri G, Liu HJ, et al. Detection of hepatitis C virus RNA sequences in B-cell non-Hodgkin lymphoma. *Am J Clin Pathol.* 2000;113(3):391-398.
17. Rickert RC, Roes J, Rajewsky K. B lymphocyte-specific, Cre-mediated mutagenesis in mice. *Nucleic Acids Res.* 1997;25(6):1317-1318.
18. Tanaka T, Lau JY, Mizokami M, et al. Simple fluorescent enzyme immunoassay for detection and quantification of hepatitis C viremia. *J Hepatol.* 1995;23(6):742-745.
19. Tsukiyama-Kohara K, Tone S, Maruyama I, et al. Activation of the CKI-CDK-Rb-E2F pathway in full genome hepatitis C virus-expressing cells. *J Biol Chem.* 2004;279(15):14531-14541.
20. Nishimura T, Kohara M, Izumi K, et al. Hepatitis C virus impairs p53 via persistent overexpression of 3beta-hydroxysterol Delta24-reductase. *J Biol Chem.* 2009;284(52):36442-36452.
21. Tsukiyama-Kohara K, Poulin F, Kohara M, et al. Adipose tissue reduction in mice lacking the translational inhibitor 4E-BP1. *Nat Med.* 2001; 7(10):1128-1132.
22. Fujimura S, Xing Y, Takeya M, et al. Increased expression of germinal center-associated nuclear protein RNA-primase is associated with lymphomagenesis. *Cancer Res.* 2005;65(13):5925-5934.
23. Miyazaki T, Kato I, Takeshita S, Karasuyama H, Kudo A. Lambda5 is required for rearrangement of the Ig kappa light chain gene in pro-B cell lines. *Int Immunol.* 1999;11(8):1195-1202.
24. Rubin LA, Galli F, Greene WC, Nelson DL, Jay G. The molecular basis for the generation of the human soluble interleukin 2 receptor. *Cytokine.* 1990;2(5):330-336.
25. Tsukiyama-Kohara K, Iizuka N, Kohara M, Nomoto A. Internal ribosome entry site within hepatitis C virus RNA. *J Virol.* 1992;66(3):1476-1483.
26. Jaffe ES, Harris NL, Stein H, Isaacson PG. Classification of lymphoid neoplasms: the microscope as a tool for disease discovery. *Blood.* 2008; 112(12):4384-4399.
27. el-Din HM, Attia MA, Hamza MR, Khaled HM, Thoraya MA, Eisa SA. Hepatitis C Virus and related changes in immunologic parameters in non Hodgkin's lymphoma patients. *Egypt J Immunol.* 2004;11(1):55-64.
28. Feldmann G, Nischalke HD, Nattermann J, et al. Induction of interleukin-6 by hepatitis C virus core protein in hepatitis C-associated mixed cryoglobulinemia and B-cell non-Hodgkin's lymphoma. *Clin Cancer Res.* 2006;12(15):4491-4498.
29. Mizuochi T, Ito M, Takai K, Yamaguchi K. Differential susceptibility of peripheral blood CD5+ and CD5− B cells to apoptosis in chronic hepatitis C patients. *Biochem Biophys Res Commun.* 2009; 389(3):512-515.
30. Bansal AS, Bruce J, Hogan PG, Prichard P, Powell EE. Serum soluble CD23 but not IL8, IL10, GM-CSF, or IFN-gamma is elevated in patients with hepatitis C infection. *Clin Immunol Immunopathol.* 1997;84(2):139-144.
31. Barrett L, Gallant M, Howley C, et al. Enhanced IL-10 production in response to hepatitis C virus proteins by peripheral blood mononuclear cells from human immunodeficiency virus-monoinfected individuals. *BMC Immunol.* 2008;9:28.
32. Rubin LA, Kurman CC, Fritz ME, et al. Soluble interleukin 2 receptors are released from activated human lymphoid cells in vitro. *J Immunol.* 1985;135(5):3172-3177.
33. Kawamura Y, Ikeda K, Arase Y, et al. Viral elimination reduces incidence of malignant lymphoma in patients with hepatitis C. *Am J Med.* 2007; 120(12):1034-1041.
34. Stamataki Z, Shannon-Lowe C, Shaw J, et al. Hepatitis C virus association with peripheral blood B lymphocytes potentiates viral infection of liver-derived hepatoma cells. *Blood.* 2009;113(3): 585-593.
35. Wasik MA, Sioutos N, Tuttle M, Butmarc JR, Kaplan WD, Kadin ME. Constitutive secretion of soluble interleukin-2 receptor by human T cell lymphoma xenografted into SCID mice. Correlation of tumor volume with concentration of tumor-derived soluble interleukin-2 receptor in body fluids of the host mice. *Am J Pathol.* 1994;144(5): 1089-1097.
36. Tsai MH, Chiou SH, Chow KC. Effect of platelet activating factor and butyrate on the expression of interleukin-2 receptor alpha in nasopharyngeal carcinoma cells. *Int J Oncol.* 2001;19(5):1049-1055.
37. Yano T, Yoshino I, Yokoyama H, et al. The clinical significance of serum soluble interleukin-2 receptors in lung cancer. *Lung Cancer.* 1996;15(1):79-84.
38. Tesarova P, Kvasnicka J, Umlaufova A, Homolkova H, Jirsa M, Tesar V. Soluble TNF and IL-2 receptors in patients with breast cancer. *Med Sci Monit.* 2000;6(4):661-667.
39. Maccio A, Lai P, Santona MC, Pagliara L, Melis GB, Mantovani G. High serum levels of soluble IL-2 receptor, cytokines, and C reactive protein correlate with impairment of T cell response in patients with advanced epithelial ovarian cancer. *Gynecol Oncol.* 1998;69(3):248-252.
40. Matsumoto T, Furukawa A, Sumiyoshi Y, Akiyama KY, Kanayama HO, Kagawa S. Serum levels of soluble interleukin-2 receptor in renal cell carcinoma. *Urology.* 1998;51(1):145-149.
41. Pountain G, Hazleman B, Cawston TE. Circulating levels of IL-1beta, IL-6 and soluble IL-2 receptor in polymyalgia rheumatica and giant cell arteritis and rheumatoid arthritis. *Br J Rheumatol.* 1998;37(7):797-798.
42. Zekri AR, Alam El-Din HM, Bahnassy AA, et al. Serum levels of soluble Fas, soluble tumor necrosis factor-receptor II, interleukin-2 receptor and interleukin-8 as early predictors of hepatocellular carcinoma in Egyptian patients with hepatitis C virus genotype-4. *Comp Hepatol.* 2010:9(1):1.
43. Sheibani K, Winberg CD, van de Velde S, Blayney DW, Rappaport H. Distribution of lymphocytes with interleukin-2 receptors (TAC antigens) in reactive lymphoproliferative processes, Hodgkin's disease, and non-Hodgkin's lymphomas. An immunohistologic study of 300 cases. *Am J Pathol.* 1987;127(1):27-37.
44. Robb RJ, Rusk CM. High and low affinity receptors for interleukin 2: implications of pronase, phorbol ester, and cell membrane studies upon the basis for differential ligand affinities. *J Immunol.* 1986;137(1):142-149.
45. Sheu BC, Hsu SM, Ho HN, Lien HC, Huang SC, Lin RH. A novel role of metalloproteinase in cancer-mediated immunosuppression. *Cancer Res.* 2001;61(1):237-242.
46. Fluckiger AC, Garrone P, Durand I, Galizzi JP, Banchereau J. Interleukin 10 (IL-10) up-regulates functional high affinity IL-2 receptors on normal and leukemic B lymphocytes. *J Exp Med.* 1993; 178(5):1473-1481.

Comparative Immunology, Microbiology and Infectious Diseases 33 (2010) e81–e88

Contents lists available at ScienceDirect

Comparative Immunology, Microbiology and Infectious Diseases

journal homepage: www.elsevier.com/locate/cimid

Evaluation of a recombinant measles virus expressing hepatitis C virus envelope proteins by infection of human PBL-NOD/Scid/Jak3null mouse

Masaaki Satoh[a], Makoto Saito[a], Kohsuke Tanaka[a], Sumako Iwanaga[b], Salem Nagla Elwy Salem Ali[a,d], Takahiro Seki[e,1], Seiji Okada[b], Michinori Kohara[c], Shinji Harada[d], Chieko Kai[e], Kyoko Tsukiyama-Kohara[a,*]

[a] Department of Experimental Phylaxiology, Faculty of Life Sciences, Kumamoto University, 1-1-1 Honjo, Kumamoto-city, Kumamoto 860-8556, Japan
[b] Division of Hematopoiesis, Center for AIDS Research, Kumamoto University, Japan
[c] Department of Microbiology and Cell Biology, Tokyo Metropolitan Institute of Medical Science, Japan
[d] Department of Medical Virology, Faculty of Life Sciences, Kumamoto University, Japan
[e] Laboratory of Animal Research Center, Institute of Medical Science, University of Tokyo, Japan

ARTICLE INFO

Article history:
Received 27 January 2010
Accepted 21 February 2010

Keywords:
MV
HCV
E1
E2
Human PBL
NOD/Scid/Jak3null mouse

ABSTRACT

In this study, we infected NOD/Scid/Jak3null mice engrafted human peripheral blood leukocytes (hu-PBL-NOJ) with measles virus Edmonston B strain (MV-Edm) expressing hepatitis C virus (HCV) envelope proteins (rMV-E1E2) to evaluate the immunogenicity as a vaccine candidate. Although human leukocytes could be isolated from the spleen of mock-infected mice during the 2-weeks experiment, the proportion of engrafted human leukocytes in mice infected with MV (10^3–10^5 pfu) or rMV-E1E2 (10^4 pfu) was decreased. Viral infection of the splenocytes was confirmed by the development of cytopathic effects (CPEs) in co-cultures of splenocytes and B95a cells and verified using RT-PCR. Finally, human antibodies against MV were more frequently observed than E2-specific antibodies in serum from mice infected with a low dose of virus (MV, 10^0–10^1 pfu, and rMV-E1E2, 10^1–10^2 pfu). These results showed the possibility of hu-PBL-NOJ mice for the evaluation of the immunogenicity of viral proteins.

1. Introduction

Hepatitis C virus (HCV) is a member of the *Flaviviridae* family and is the causative agent of both chronic hepatitis and hepatocellular carcinoma (HCC) [1–3]. 170 million people are infected with HCV worldwide [4,5]. Despite prevention efforts and advanced treatment strategies, including combined PEGylated alpha interferron (PEGIFN-α) and ribavirin therapy [6,7], the clinical efficacy of this treatment is limited [8,9]. Alternative novel antiviral agents that have been shown to elicit effective responses in chronically infected patients, such as inhibitors of viral protease, helicase, and polymerase, are currently being developed but are expensive [10]. Therefore, the development of an effective vaccine that either induces the production of high-titer, long-lasting, and cross-reactive neutralising antibodies or induces a cellular immune response is important.

Immunological approaches to control HCV infection have proven to be ineffective, in part because HCV adapts to escape from the host immune system [11]. Furthermore, a high percentage of immunocompetent individuals

* Corresponding author. Tel.: +81 96 373 5560; fax: +81 96 373 55620.
E-mail address: kkohara@kumamoto-u.ac.jp (K. Tsukiyama-Kohara).

[1] Present address: Virology, Shionogi Research Laboratories, Shionogi & Co Ltd, Osaka, Japan.

0147-9571/$ – see front matter © 2010 Elsevier Ltd. All rights reserved.
doi:10.1016/j.cimid.2010.02.006

are infected by HCV despite their ability to mount an active immune response [12]. A preventive HCV vaccine is required to protect unexposed individuals from HCV infection. This vaccine will most likely need to target the viral envelope glycoprotein, E1 and E2, and must also be bivalent, safe, and provide long-lasting protective immunity. To address this challenge, we evaluated the immunogenicity of a live-attenuated recombinant vector derived from the pediatric measles virus (MV) that expresses HCV antigens. The MV vaccine is a well-known, live-attenuated vaccine and has proven to be one of the safest, most stable, and effective human vaccines [13]. This vaccine is produced on a large scale in many countries and used at low cost through the Extended Program on Immunisation of the WHO [14,15]. While this vaccine has been shown to induce life-long immunity with a single dose, boosting is effective. Efforts to develop vaccines using recombinant MV expressing different proteins derived from dengue virus [16,17], human immunodeficiency virus (HIV) [18–21], Human papilloma virus (HPV) [22], Severe acute respiratory syndrome (SARS) [23], or West Nile virus (WNV) [24] have been described. We constructed a recombinant MV expressing the E1 and E2 envelope glycoproteins of HCV (rMV-E1E2) [25] and demonstrated that this virus could infect B95a cells and express HCV E1.

HCV research has long been hampered by the lack of an animal model that reproduces HCV infection in humans. The model in which severe combined immunodeficient (SCID) mice are transplanted with human peripheral blood leukocyte (PBL) is a well-established system to study human immunity (hu-PBL-SCID). This mouse develops all human lymphoid cell lineages that repopulate the animal's lymphoid organs. Our group previously generated the non-obese diabetic (NOD)/SCID/Janus kinase 3 (Jak3) knockout (NOJ) mouse model and then established a human hemolymphoid system in this mouse [26,27]. In this study, we infect human PBL-transplanted NOJ mice with MV and rMV-E1E2 and then characterise the humoral immune responses elicited by the transplanted human cells, in order to evaluate rMV-E1E2 as a vaccine candidate.

2. Materials and methods

2.1. Cells

B95a cells, a marmoset B cell line [28], were used for viral titration and rescue, and were maintained in RPMI 1640 medium supplemented with 10% heat-inactivated foetal calf serum (FCS).

2.2. Plasmid construction and viral rescue

The cDNAs encoding HCV E1 and E2 were obtained from the plasmid HCR6CNS2 [29]. We used replication-competent MV-based vectors (pMV; Edmonston B strain of MV) [25]. The E1 and E2 cDNAs were cloned into the *Fse* I site of pMV and the resulting clone, pMV-E1E2, was used to rescue the infectious recombinant MV expressing the HCV envelope glycoproteins (rMV-E1E2), as reported previously [30].

2.3. Generation of humanised mice

Mice were reconstituted as described previously [26,27]. The NOD/SCID/JAK3^{null} strain was established by backcrossing JAK3^{null} and the NOD Cg-Prkdc^{Scid} strains for ten generations. All animal experiments were performed according to the guidelines of Institutional Animal Committee or Ethics Committee of Kumamoto University.

2.4. Preparation of human blood leukocytes and transplantation

Peripheral blood leukocytes were isolated from blood donors using Ficoll–Hypaque density gradient centrifugation. A total of 5×10^6 cells were transplanted into the spleen of irradiated (2 Gy) 4-week-old mice.

2.5. MV and MV-E1E2 infection

We injected 10^0–10^5 pfu of MV or 10^0–10^2 or 10^4 pfu of MV-E1E2 intraperitoneally for MV and MV-E1E2 infection, respectively. As a negative control, a group of mice was injected with RPMI 1640. Mice were monitored for 2 weeks and then euthanised. The spleens and peripheral blood were collected for analysis.

2.6. Flow cytometry

Isolated splenocytes were stained with APC-Cy7-conjugated anti-mouse CD45 (BD Pharmingen) to detect the murine leukocytes and either APC- or pacific blue-conjugated anti-human CD45 (DAKO) to detect human leukocytes. All data were analysed using FlowJo (Tree Star).

2.7. Confirmation of viral infection

The viral infection of the human leukocytes was confirmed using co-culture with B95a cells followed by RT-PCR. Suspensions of isolated splenocytes were co-cultured with B95a cells and the formation of cytopathic effects (CPEs) was monitored for 2 weeks. Additionally, RNA was isolated from the supernatant of the co-cultures using ISOGEN-LS (Nippon gene) according to manufacturer's instructions. MV RNA was detected using reverse transcript-PCR (RT-PCR) with the sense primer, 5′-ACTCGGTATCACTGCCGAGGATGCAAGGC-3′ (1256–1284) and anti-sense primer 5′-CAGCGTCGTCATCGCTCTCTCC-3′ (2077–2056) or 5′-atggcagaagagcaggcacg-3′ (1807–1826). HCV E1 or E2 was amplified using E1-S-1051 5′-ccgttgctgggtggcactta-3′ and E1-AS-1314 5′-atcatcatgtcccaagccat-3′ or E2-S-1600 5′-ctggcacatcaacaggactg-3′ and E2-AS-1960 5′-aaggagcagcacgtctgtct-3′.

2.8. ELISA

Anti-MV antibody titers were determined by using an ELISA assay. 96-well plates were coated with a 25 μg/ml solution of MV-infected B95a lysate or recombinant E2-expressing baculovirus-infected Sf9 lysate as antigen, respectively. The plates were consecutively incubated with

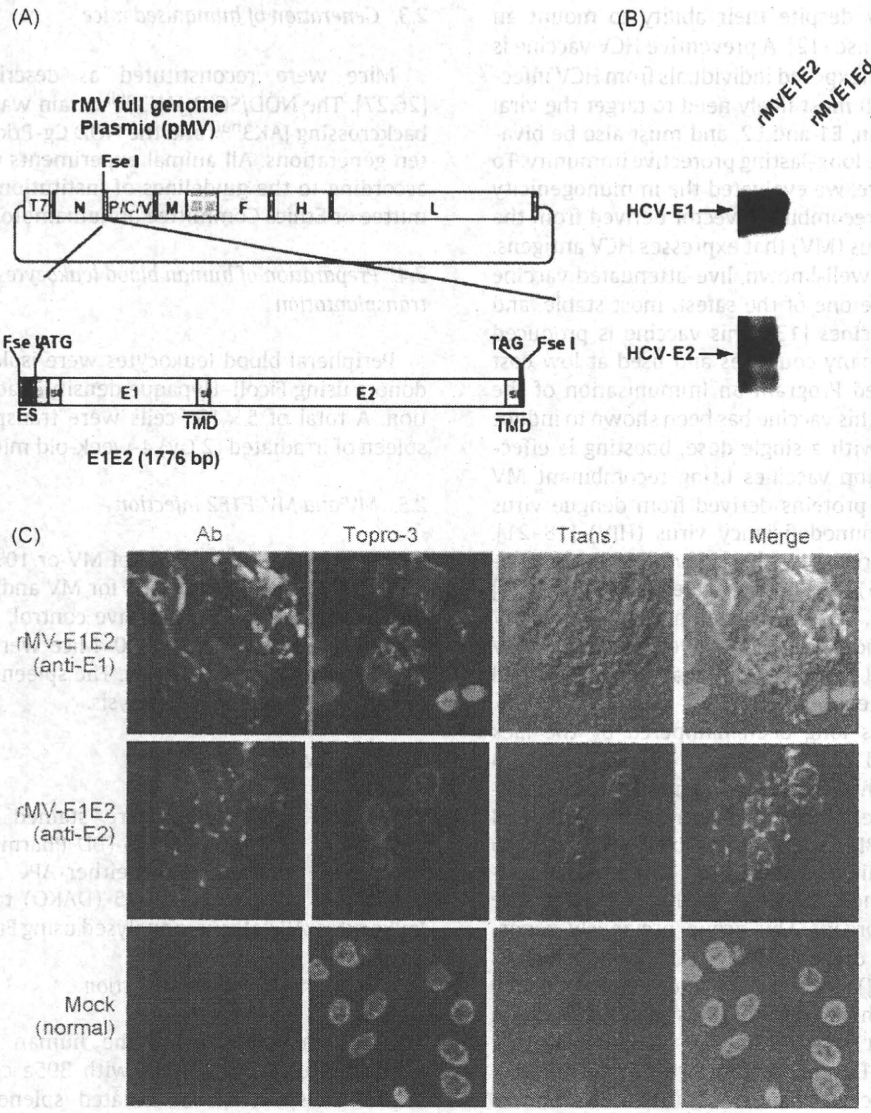

Fig. 1. Construction of the recombinant MV vectors. (A) The rMV full genome vector derived from the MV-Ed strain is illustrated in the upper panel and is labelled with letters as follows: N, nucleocapsid; P, phosphoprotein; M, matrix; F, fusion; H, hemagglutinin; and L, large. T7 indicates the T7 RNA polymerase promoter. The cDNA encoding the HCV envelope glycoproteins (E1 and E2) containing the signal peptide sequence (SP) and the transmembrane domain (TMD, underlined) regions, the N gene end signal (E), the P gene start signal (S), and the intercistronic region of the H protein genes at the 5′ end, which was flanked by Fse I sites at both ends, was introduced into the unique Fse I site in between the N and P genes in the pMV vector. The resulting plasmid was designated pMV-E1E2. (B) The HCV E1 and E2 proteins were detected in rMV-E1E2-, rMV-Ed- and mock-infected B95a cells by western blot with MoAb 384 and 544 (arrows). (C) rMV-E1E2-infected B95a cells were stained with MoAb 299 (anti-E1) or MoAb 187 (anti-E2) and analysed by immunofluorescence. Nuclei were stained with Topro-3 and the bright field and merged images are indicated (400×).

sera (1:100) recovered from hu-PBL-NOJ mice, peroxidase-conjugated rabbit-human IgG (DAKO), and TMB Peroxidase EIA Substrate Kit (Bio-Rad) at 37 °C for 1 h. Optimal density values were measured at 450 nm.

An anti-MV-NP antibody (Millipore, MA, USA) and normal mouse serum (NMS) were used as positive control and negative control respectively.

2.9. Western blot analysis

Total protein extracts from E2-expressing baculovirus-infected Sf9 lysate were separated by SDS-PAGE. The primary antibodies used for Western blots were as follows: sera from mice (1:100) and anti-E2 monoclonal antibody (1:5000). Peroxidase-conjugated secondary antibodies were added and incubated with the mixture for 1 h at room temperature.

3. Results

3.1. Construction of recombinant measles virus expressing E1 and E2

The HCV genes corresponding to the envelope proteins E1 and E2 were sub-cloned in between the N and P genes of the MV vector (Fig. 1A). The HCV E1 and E2 genes included

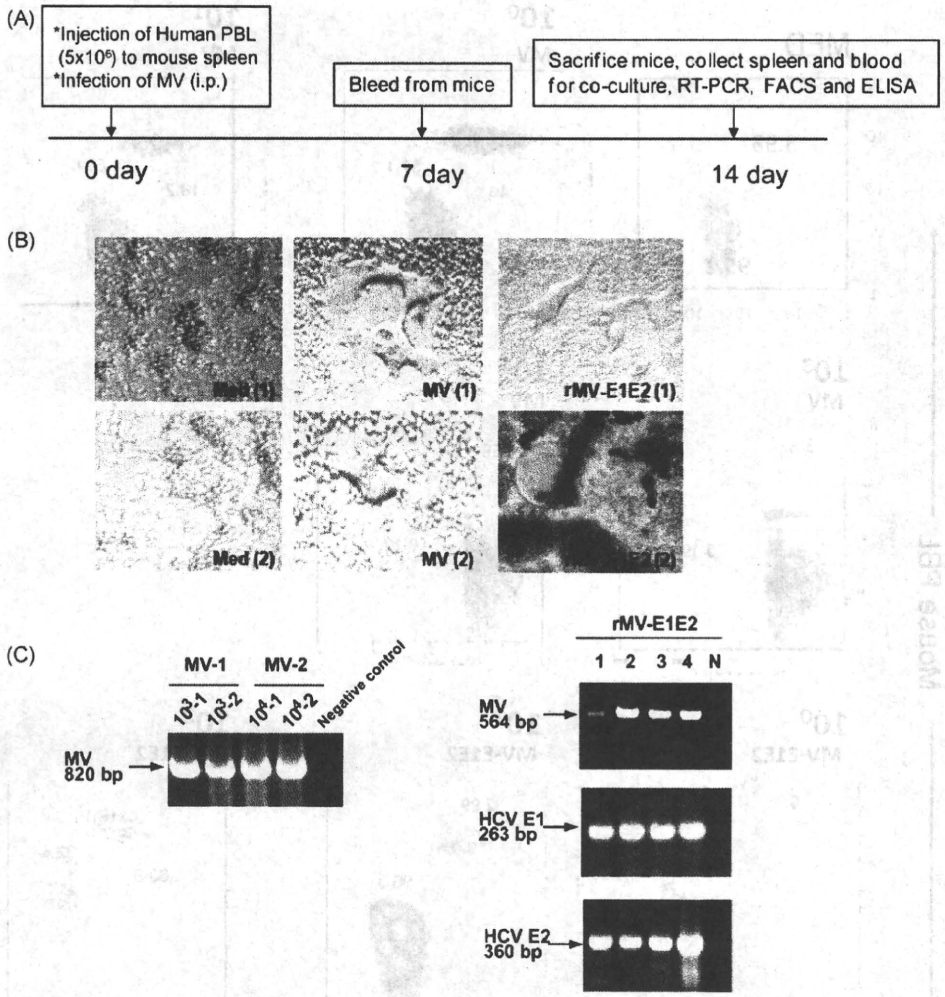

Fig. 2. Infection of hu-PBL-NOD/Scid mice with rMV and rMV-E1E2. (A) Course of infection of hu-PBL-NOD/SCID mice with MV and rMV-E1E2. (B) CPE formation in co-cultures of splenocytes isolated from MV- (MV1, 2), rMV-E1E2-, or mock-infected hu-PBL-NOD/SCID and B95a cells (40× magnification). (C) Detection of viral RNA by RT-PCR. Detection of MV in MV-1- or 2-infected mouse splenocyte co-cultures (820 bp) and rMV-E1E2-infected splenocyte co-cultures (564 bp), and HCV E1 (263 bp) and E2 (360 bp) in rMV-E1E2 (10^4 pfu)-infected splenocyte co-cultures (arrows).

the putative signal peptide sequences at the N terminus and the transmembrane domain at the C terminus [31]. The plasmid vector pMV-E1E2 was introduced with supporting plasmids into 293T cells to rescue the recombinant viruses. The expression of the E1 and E2 proteins by rMV-E1E2 was examined by Western blot (Fig. 1B) and immunofluorescence (Fig. 1C).

3.2. Infection of hu-PBL-NOJ mice with MV and rMV-E1E2

All hu-PBL-NOJ mouse infections were observed for 14 days (Fig. 2A). Infections with MV and rMV-E1E2 were confirmed by first co-culturing the human leukocytes isolated from the spleens of infected mice with B95a cells and then verifying the presence of virus by RT-PCR. In all the MV (10^3–10^4 pfu) or rMV-E1E2 (10^4 pfu)-infected hu-PBL-NOJ mice, CPEs were observed in co-cultures with splenocytes (Table 1; Fig. 2B). The results of the co-culture assays are in agreement with results that were obtained by RT-PCR; positive bands were observed in the mice infected with 10^3–10^4 pfu of MV and 10^4 pfu of rMV-E1E2 (Fig. 2C). These results demonstrate that the rescued MV and rMV-E1E2 are able to infect transplanted human PBL.

Table 1
Summary of MV and MV-E1E2 infection of hu-PBL-NOJ mice.

Virus	Amount of virus (PFU)	No. tested	CPE	RT-PCR
Mock	Medium	7	0/7	0/7
MV	10^0	3	0/3	0/3
	10^1	3	0/3	0/3
	10^2	3	0/3	0/3
	10^3	2	2/2	2/2
	10^4	2	2/2	2/2
MV-E1E2	10^0	3	0/3	0/3
	10^1	3	0/3	0/3
	10^2	3	0/3	1/3
	10^4	4	4/4	4/4

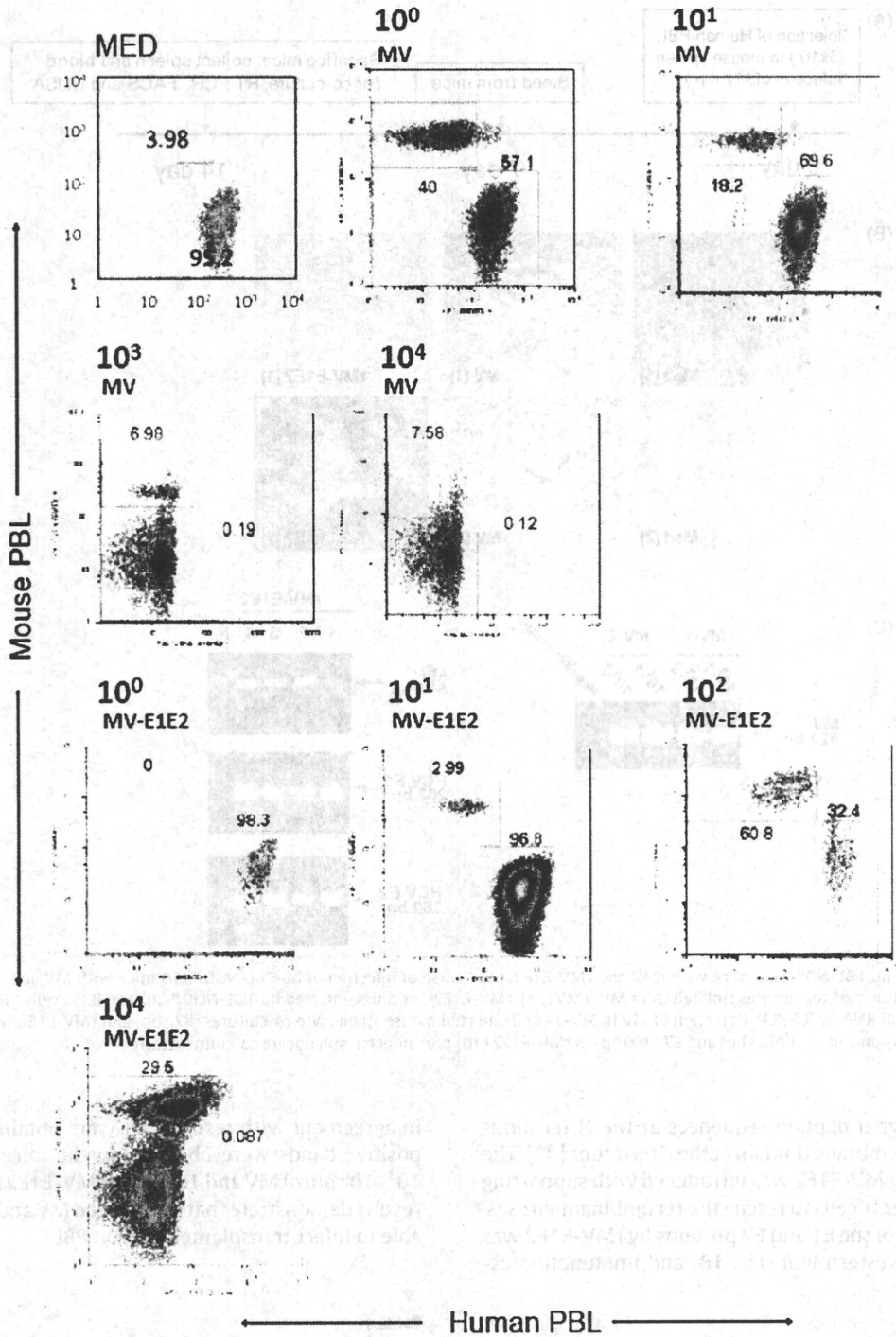

Fig. 3. Flow cytometric analysis of splenocytes isolated from hu-PBL-NOJ mice inoculated with medium, MV-Ed (10^0–10^4 pfu), or rMV-E1E2 (10^0–10^2 or 10^4 pfu). Splenocytes, consisting of both human and murine cells, were stained with antibodies against human or mouse CD45. Representative flow cytometric profiles of each group of infected mice are shown. The percentages of mouse and human leukocytes are shown.

3.3. Proportion of engrafted human leukocytes in MV- and rMV-E1E2- infected hu-PBL-NOJ mice

We also examined the splenocytes of infected mice simultaneously, using flow cytometry to determine the proportion of human cells in the spleen (Fig. 3, Table 2). In the MV-infected hu-PBL-NOJ mice, a population of human leukocytes was observed in the mice that were infected with 10^0–10^1 pfu, whereas few human leukocytes were observed in mice infected with 10^2–10^4 pfu. In contrast, in the rMV-E1E2-infected mice, a population of human leukocytes was detected in mice that were inoculated with 10^0–10^2 pfu. The ratio of human leukocytes settlement in both groups of mice was inversely correlated

Table 2
Proportion of human peripheral leukocytes in the spleen of MV-, rMV-E1E2, or mock-infected hu-PBL-NOJ mice.

Virus	Amount of virus (PFU)	No. tested	huPBL settlement (average ± S.D.%)
Mock	Medium	6	90.9 ± 13.1
MV	10^0	3	92.7 ± 11.2
	10^1	3	58.4 ± 50.6
	10^2	3	55.1 ± 49.9
	10^3	4	4.9 ± 6
	10^4	2	1.7
MV-E1E2	10^0	2	79.6
	10^1	2	96.0
	10^2	3	56.2 ± 36.2
	10^4	3	0.34 ± 0.4

with the results from the RT-PCR and co-culture assays (Table 1).

3.4. Humoral response of MV- and rMV-E1E2-infected hu-PBL-NOJ mice

To examine the immune response against MV and rMV-E1E2 by the transplanted human PBLs, we measured human MV- or HCV-specific antibodies using an ELISA with an MV-infected B95a cell lysate (Fig. 4A) or recombinant HCV E2 protein (Fig. 4B). A significant amount of human antibody against MV antigens was detected in the sera from mice that were infected with MV (10^0–10^1 pfu) or rMV-E1E2 (10^1–10^2 pfu) (Fig. 4A and B). However, only one mouse, which was infected with 10^2 pfu of rMV-E1E2, generated human antibodies against HCV E2 (Fig. 5A). The antibody responses in this mouse were confirmed by Western blot analysis (Fig. 5B).

4. Discussion

The development of a vaccine against HCV has relied on several tools, including recombinant proteins and peptides that are derived from HCV antigens [12,32–34]. HCV E1 E2 proteins play essential roles in the entry of HCV into host cells. Therefore, these proteins represent ideal targets for neutralising antibodies to block viral entry.

Several studies have used the measles virus as a vector for expression of other viral proteins [16,17]. In this study, we examined the infectivity of a rescued Edmonston B strain of MV and a recombinant rMV-E1E2 that was constructed using reverse genetics [25,30]. We demonstrate that these viruses can infect hu-PBL-NOJ mice. This is the first report demonstrating that rescued virus, including a recombinant virus, can infect hu-PBL-NOJ mice. Furthermore, an adequate viral titer could control the generation of antibodies in these mice. Based on the flow cytometry data, most of the human leukocytes disappeared following infection with high virus titer (10^3–10^4 pfu) and human antibody was not detected in these mice (data not shown). In contrast, a population of human leukocytes was detected in the mice that were inoculated with a lower dose of virus (10^0–10^2 pfu). In addition, we could detect human antibodies in the serum of mice that were infected with a low dose of virus, suggesting that this viral titer range is suitable for the induction of an antibody response that targets rMVs in the hu-PBL-NOJ mouse system. This range of virus concentration is adequate for antibody production and the resulting antibody response might suppress the viral growth of 10^0–10^1 pfu MVs in hu-PBL-NOJ mice.

The humanised mouse is a promising model for studying the transmission of the live, attenuated Edmonston B strain of the measles virus. There have been several reports detailing the infection of experimental transgenic mice that

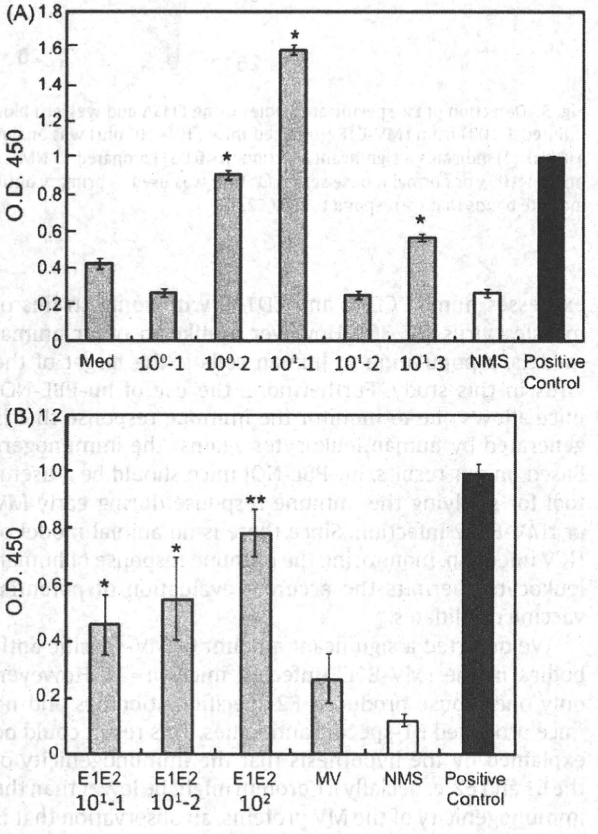

Fig. 4. Detection of human MV-specific antibodies in the serum of rMV- or rMV-E1E2-infected mice. (A) Serum (1:100) from MV-infected mice (10^0–10^1 pfu) was analysed by ELISA using an MV-infected B95a cell lysate as the target. An anti-MV-NP antibody was used as a positive control and NMS indicates normal mouse serum. The asterisk (*) indicates a significant reaction ($p < 0.01$) compared to the medium alone control. (B) Serum (1:100) from rMV-E1E2-infected mice (10^1–10^2 pfu) was analysed by ELISA. An anti-MV-NP antibody was used as a positive control and NMS indicates normal mouse serum. The double asterisk (**) indicates a highly significant reaction ($p < 0.001$) compared to NMS and a single asterisk (*) indicates a significant reaction ($p < 0.05$) compared to NMS.